DETERMINATION OF SENSITIVITY AND RELIABILITY OF NDI TECHNIQUES ON DAMAGE TOLERANCE BASED LIFE PREDICTION OF TURBINE DISCS

A Master's Thesis

Presented by

Mehmet ŞİMŞİR

to

the Graduate School of Natural and Applied Sciences

of Middle East Technical University

in Partial Fulfillment for the Degree of

MASTER OF SCIENCE

in

METALLURGICAL ENGINEERING

MIDDLE EAST TECHNICAL UNIVERSITY

ANKARA

January, 1995

Approval of the Graduate School of Natural and Applied Sicences.

Prof. Dr. İsmail Tosun

for Director

I certify that this thesis satisfies all the requirements as a thesis for the degree of Master of Science.

Prof. Dr. Mustafa Doruk

Chairman of the Department

We certify that we have read this thesis and that in our opinion it is fully adequate, in scope and quality, as a thesis for the degree of Master of Science in Metuallurgical Engineering.

Prof. Dr. Alpay Ankara

Supervisor

Examining Committe in Charge:

Prof. Dr. Mustafa DORUK

Prof. Dr. Alpay ANKARA

Doç. Dr. Filiz SARIOĞLU

Doç. Dr. Rıza GÜRBÜZ

Yr. Doç.Dr. Bilgehan ÖGEL

ABSTRACT

DETERMINATION OF SENSITIVITY AND RELIABILITY OF NDI TECHNIQUES ON DAMAGE TOLERANCE BASED LIFE PREDICTION OF TURBINE DISCS

ŞİMŞİR, Mehmet

M.S. in Metallurgical Engineering

Supervisor: Prof. Dr. Alpay Ankara

January, 1995, 68 pages

In this study, two Non-Destructive Inspection (NDI) methods have been used to determine the Damage Tolerance Life Prediction" of aero-engine turbine discs. For this purpose, low cycle fatigue cracks were examined in the compressor discs of tie bolt holes. The succesful implementation of Damage Tolerance Design Method strongly depends on the sensitivity and reliability of applied NDI method.

The result of this study indicated that the Manual Eddy Current Inspection Method is more sensitive and more reliable than the Liquid Penetrant Inspection Method interms of detection of small cracks in the compressor discs.

Key Words: LPI and Eddy Current Inspection Techniques, Sensitivity and Reliability of NDI Techniques, Damage Tolerance Design Method.

Science Code: 604.02.06

ÖZ

TÜRBİN DİSKLERİN ÖMÜRLERİN HASAR TOLERANS METODUNA GÖRE HESAPLANMASINDA TAHRIBATSIZ MUAYENE TEKNİKLERİNİN HASSASLIĞININ VE GÜVENLİLİĞİNİN TESPİT EDİLMESİ

ŞİMŞİR, Mehmet

Yüksek Lisans Tezi, Metalurji Mühendisliği

Tez Yöneticisi: Prof. Dr. Alpay Ankara

Ocak, 1995, 68 sayfa.

Bu çalışmada, Uçak Motorlarındaki turbin disk ömürlerini "Hasara Toleranslı" dizayn yöntemine göre hesaplanabilmesi için iki Tahribatsız Muayene yöntemi kullanılmıştır. Bu amaçla disklerin civatta deliklerinde oluşan yorulma çatlakları incelendi. Hasara Toleranslı Dizayn Yönteminin başarılı bir şekilde uyğulanması, uygulanan Tahribatsız Muayene Yönteminin hassaslığına ve güvenilirliliğine bağlıdır.

Bu çalışmanın sonunda el kumandalı Girdap Akımları Yöntemi Kompressör disklerindeki yorulma çatlaklarının tesbitinde Sıvı Penetrant Yönteminden daha hassas ve güvenilir olduğu ortaya kondu.

Anahtar Kelimeler: Girdap Akımı, Sıvı Penetrant Yöntemleri, Hasara Toleranslı Dizayn Yöntemi, Tahribatsız Muayene Tekniğinin Hassasiyeti ve Güvenliliği.

Bilim Kodu: 604.02.06

ACKNOWLEDGEMENTS

I would sincerely like to thank my supervisor Prof. Dr. Alpay ANKARA for his support and kind assistance which was much appreciated. I would also like to extend my gratitude to Deniz DİKMEN for her appreciated guidance. A special thanks is also extended to Mr. F. GRIENER of the Welding and Non-Destructive Center of METU for the detailed information he has supplied which has made an exclusive contribution to my thesis. Also, a thanks is extended to Cengiz TAN for his assistance.

TABLE OF CONTENTS

Page

Page

Page

APPENDICES

LIST OF TABLES

Page

LIST OF FIGURES

Page

Page

LIST OF SYMBOLS

a	Crack Size, mm
a_d	Dysfunction Size, mm
ASTM	American Society for Testing and Materials
C	Experimental Material Constant
CLM	Confidence Limit Measurement
DFM	Deterministic Fracture Mechanics
DTLP	Damage Tolerance Life Prediction
FCGR	Fatigue Crack Growth Rate
HCF	High Cycle Fatigue
ΔK	Stress Intensity Factor
LEFM	Linear Elastic Fracture Mechanics
NDE	Non-Destructive Evaluation
NDI	Non-Destructive Inspection
N_d	Number of Cycle at he Dysfunction Size
n	Experimental Material Constant
OPM	Optimized Probability Method
p	Probability of False Call Indication
PFM	Probabilistic Fraction Mechanics
Pi	Probability of Indication at i
POD	Probability of Detection
POI	Probability of Indication
RFC	Retirement for Cause
RIM	Range Interval Method

SII	Safe Inspection Interval
$S_{\Delta\sigma}$,Sc,Sa	Standard Deviation
$\Delta\sigma$	Stress Amplitude
Sy/xs	Condition Standard Variance
λ_1	Mean
λ	Shape Factor
ζ	Standard Deviation of Variate
η	Characteristic Life
β	Slope
β_0	Location Parameter
β_1	Slope Parameter

CHAPTER I

INTRODUCTION

Fracture Control Philosophies are used in the design and development and life prediction of mainly highly stressed components. Components of a structure are removed from service when they have reached an operational cycle determined by fracture control design method. A common applied life prediction method is the 'Safe Life Prediction Method'. However, the most of the retired components still have useful life and so they will not be fully utilized when they are designed according to safe life prediction method. For this reason, the cost and logistics associated with spare part replacement under safe life philosophy are high and according to this philosophy the material is free of initial defects. There were many failed engines which have been designed based on safe life limit. Due to the expensive maintenance costs for the 'Safe Life Limit and its Philosophy' an alternative design method has been developed to assure safe use of the components beyond the period of Safe Life Limit.

A new implementation for the maintenance philosophy known as 'Retirement For Cause' (RFC) has been established by the US Air Force. The RFC approach is based on a 'Damage Tolerance' design philosophy and according to this philosophy, all components contain flaws. By using routine inspections by Non-Destruction Inspection Methods and Fracture Mechanics predictions, the Damage Tolerance approach ensures that flaws will not grow to critical size during service.

In order to apply the Damage Tolerance Design Philosophy, it is required that the NDI procedures are seen to be quantified in terms of their sensitivity and reliability which are defined by Probability of Detections (POD) and their Confidence Limit Measurements (CLM).

The aim of this study is to determine which NDI method (i.e. Eddy Current Inspection and Liquid Penetrant Inspection) is suitable for Damage Tolerance Based Life Prediction of aero-engine turbine discs according to degree of reliability and the level of sensitivity of NDI methods.

The probability of detection of NDI procedures can be assessed experimentally by inspecting statistically valid number of flawed and flaw-free parts.

1.1 Overview to Developments on Damage Tolerance Design

In recent years aircraft structures have progressed significantly i.e. Weight of Materials used in aero-engine have decreased while their strength and resistance to crack propagation is increased. These results have been obtained by means of more sophisticated designs, advanced technology of materials and improved correlations between laboratory tests and full scale inspection.

It is necessary to throughly examine the basic concepts of the progess where NDI plays a fundamental role.

The NDI methods are specified for component inspection requirements in order to maintain the necessary quality for the final service of life of the

component. In most industries, the inspection requirements are defined in a specification which identifies the sensitivity level of the inspection method as well as the flaw size. Each and every specification defines a procedure which demonstrates the capability to reject against defects at the point of the required sensitivity level. As an example, the AMS 2630 A specification, defines the calibration technique used to set up the ultrasonic instrumentation.

Ultrasonic standards have been designed to identify and follow through the performance of the inspection system. Specific procedures have been defined by the 'American Society for Testing and Materials' (ASTM) for the manufacture of the ultrasonic reference blocks for Longitudinal Wave Testing [Ref. 26 and 27].

After several catastrophic failures of the major engineering systems (for example; the F111, space shuttle, nuclear reactors and the Alaskan pipeline) and the development of high technology materials such as, composites has created major forces in the development and application of NDI technology [Ref. 20]. The specification requirements are designed to control the inspection processes and the quality of the inspection results.

Nevertheless, a new design method using Linear Elastic Fracture Mechanics (LEFM) required inspection methodology for detection defects in production and in service. LEFM design assumes the presence of structural defects and then allows the designer to ensure the following questions:

1. What will be the critical flaw size that will cause failure in a given component which is subjected to service stress and temperature conditions?

2. How long can a precracked structure be safely operated in service?

3. How can a structure be designed to prevent catastrophic failure from pre-existing cracks?

4. What inspections must be performed to prevent catastrophic failure?

The ability to answer these questions forms the basis of Non-Destructive Evaluation (NDE). The NDE involves damage tolerance design approach and is centered on the philosophy of ensuring safe operation in the presence of flaws.

The function mentioned above may cause the NDE/NDI to evaluate the inspection of capabilities and sensitivities. The first evaluation in the aerospace industry was conducted by Lockheed in the 1970's and was called "How Cracks will Travel" programme [Ref . 14]. Many advancements have been made in NDE/NDI technology to improve the inspection capability since that stage of inquiry.

CHAPTER II

THE ROLE OF NDI TECHNIQUES ON DAMAGE TOLERANCE DESIGN OF AN AIRCRAFT ENGINE COMPONENTS

The useful life of aircraft engine components, such as discs and spacers, are not used to its full capacity through the facilitation of a safe life design approach. This is due to the fact that only few (eg. 1 in 1000) components have developed a crack of detectable size at retirement [Ref. 2 and 21]. Therefore, alternative design and life cycle management procedures based on damage tolerance concepts are currently being considered for several new and existing engines. The damage tolerance design approach was first introduced by the USAF in 1970, and this new approach has been effectively applied since 1970 on a number of civil and military aircrafts (MLT-STD-1530 and MIL-A83444). Nevertheless, damage tolerant design has been a recent development for engine components. The application of this design approach, with respect to disc lifing, is currently under consideration and occasionally is applied. Another new specification on engine damage tolerance requirements, has recently been developed and this has been listed as MIL-STD-1783.

Most discs are currently designed upon the safe-life philosophy. Both design approaches which were mentioned so far are listed below.

2.1 Safe Life Design

The safe life design is still one of the most widely used approach in the lifing of engine discs. In this respect, "Safe Life" means that parts are designed for a service life for which no significant damage will occur. No defects are assumed to occur before reaching the safe life limit.

With respect to aircraft engine discs, the safe life is defined as the number of cycles at which one of every 1000 components will develop a crack of 0.8 mm surface length. This crack size has been chosen because;

(1) at this size, high cycle fatigue (HCF) crack growth under vibrating conditions do not occur,
(2) this crack size for existing materials is significantly smaller than the critical crack size, and
(3) a 0.8 mm crack is considered to be the smallest crack detectable.

The Safe Life Design of discs implies that 999 out of 1000 components are rejected based on statistical probability of a crack forming without requiring the presence of a detectable crack. From economic consideration, this is not attractive. It has been shown (Ref. 19 and 22) that a large scatter in time to initiate and grow a crack to a detectable size, most of these removed components have considerable service life. If components could be removed from service according to presence of actual crack, this inherent available life would be used much better. This later consideration is the basis of damage tolerance design philosophy.

2.2 Damage Tolerance Design

As it was noted before that in most of the engine aparatuses the usefull life of the components is not fully utilized because of the Safe Life Approach. Therefore, alternative life design methods have been considering for engine components. Damage Tolerance forms the fundamentals of this design philosophy.

Damage Tolerance is defined as the ability of an engine to resist failure due to presence of cracks or other defects for a specified period of usage.

To be able to apply the Damage Tolerance Design Method, it is required to know some design parameters;

* Operational load history of component.
* Materials crack growth data for operational loading conditions (Ref. 17).
* The suitability of NDI or other techniques for the reliable detection of very small cracks.

Several systems are used for monitoring operational load parameters e.g. the Aircraft Integrated data and the Engine Usage Monitoring System (Ref. 16).

In theory, Damage Tolerance philosophy assumes that critical location of a component contains cracks and size of those cracks is just below detection limit of the NDI techniques used to inspect the component. Also, it assumes that crack grows in the service in a way and this can be identified by LEFM or other Fracture Mechanics. When the predetermined Crack Length Limit is reached, there will be a risk of failure due to possible rapid crack growth (Ref. 2). This predetermined crack

length is known as 'Dysfunction Limit' and it is calculated by fracture mechanics analysis and a safety factor as given by the engine manufacturers.

A damage tolerance approach ensures that the initial crack does not grow beyond its dysfunction size. This is done by calculating the number of fatigue cycles to dysfunction and by imposing inspection intervals shorter than the time interval necessary for the crack to grow from its initial size to dysfunction. The damage tolerance lifing approach is indicated in Figure 1. As it can be seen that regular inspection may screen out components which have insufficient life to be returned to service.

The damage tolerance approach is used to calculate the number of hours (or cycles) to dysfunction. However, predictions are strongly influenced by the initial and dysfunction crack length values used in the calculations. The dysfunction crack size is determined by using the estimates of service loads and material properties on the worst case service conditions for a given component. On the other hand, the initial crack length depends strongly on the detection and sizing capabilities of nondestructive inspection (NDI) technique used to inspect the components. The NDI technique requires to be quantified in terms of crack detection capabilities (sensitivity) and reliability (probability of detection) in order to establish the most suitable NDI technique for the use in damage tolerance life predictions. A valid demonstration programme is used to assess the suitability of a given NDI technique. The flawed and flaw free parts are inspected by NDI procedures that duplicate the maintenance inspections.

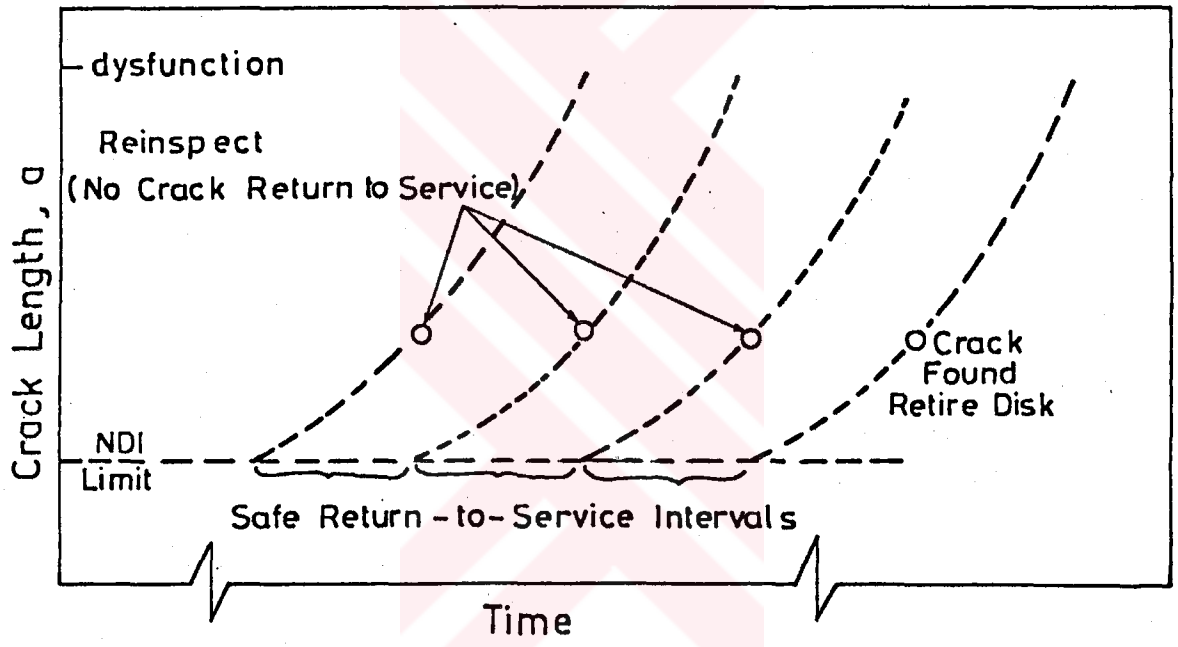

Figure 1. Schematic of Damage Tolerance Lifing Approach

This thesis shall describe the procedures used for nondestructive inspections of compressor discs as well as the statistical analysis used to obtain probability of detection curves and 95% lower confidence bounds.

2.2.1 Deterministic Fracture Mechanics

The number of cycles which are required to grow the assumed crack (a_i) to its dysfunction size (a_d) is used to define a safe inspection interval (SII) usually by dividing the life to dysfunction by a safety factor 2 [Ref. 12]. This life cycle managements concept is illustrated in Figure 1. Figure 1 shows that at the end of one SII, all components are inspected and crack free components are returned to service for another SII. This procedure is repeated until a crack is found. Components are retired on an individual basis when their condition dictates. In order to implement the DTLP procedure as diplayed in Figure 1, it is possible to determine the detection limits of the candidate NDI techniques and to ensure that the selected NDI technique does not miss a dysfunction crack size under any circumstances. It has been specified by the United State Air Force (USAF) MIL-STD-1783 that initial flaws can be assumed to exist as a result of material manufacturing and processing operations and that these flaw sizes are based on the material defect distribution, manufacturing process and NDI methods to be used during manufacture of the component [Ref. 25].

In practice, the SII is computed either by using Deterministic Fracture Mechanics (DFM) or Probabilistic Fracture Mechanics (PFM) approached [Ref. 8, 12 and 23]. The DFM approach assumes that an initial flaw size a_i already exists in the critical location of the component, whereas a_i is defined as the maximum crack size which is missed by the NDI technique used [Ref. 25].

Fracture Mechanics analysis is carried out in order to plot the curve of the most damaged crack size (a) versus the number of fatigue cycles as displayed in Figure 1. The cyclic stress intensity factor (ΔK) of the crack tip is given by;

$$\Delta K = \Delta\sigma\sqrt{\lambda\pi a} \quad (1)$$

where λ is a factor which depends on the crack shape, structure and gradient of stresses and Δσ is the stress amplitude. If the stable fatigue crack growth conditions prevail, the Fatigue Crack Growth Rate (FCGR) is given by;

$$\frac{da}{dN} = C.(\Delta K)^n \quad (2)$$

where C and n are experimental material constants. Upon substituting for ΔK from equation (1) in equation (2) and integrating, the number of fatigue cycles (N_d) required to grow a crack from the assumed initial size a_i to dysfunction size a_d is given by;

$$Nd = \frac{1}{C\left(\Delta\sigma\sqrt{\pi}\right)^n}\int_{a_i}^{a_d}(\lambda a)^{\frac{n}{2}}da \quad (3)$$

However, the DFM approach can be calculated by using worst case values of n, C, Δσ, a_i and a_d, where SII is;

$$SII = \frac{N_d}{2} \quad (4)$$

It can be seen that for each and every variable in equation (3) may not occur in real life and that the above assumptions may impose unrealistic contraints on SII calculation [Ref. 7 and 18] and DFM approach which is used to calculate the N_d.

2.2.2 Probabilistic Fracture Mechanics

The Probabilistic Fracture Mechanics (PFM) approach uses deterministic equations (1) to (4) for calculating a SII but input parameters such as a_i, a_d, C, n, and $\Delta\sigma$ are random variables with known or assumed distributions to generate a N_d distribution curve [Ref. 6, 8 and 18]. Therefore, rather than calculating a single SII value and using a safety factor, a range of SII's is calculated and appropriate values are selected to maintain a sufficiently low and a cheaper failure probability (F). For example, the observed scatter in da/dN in equation (2) could be simulated by random variation in C, for which C is assumed to show a log-normal distribution [Ref. 18].

$$\text{or} \qquad \log C = \text{Gau}\,(\mu_c, S_c) \tag{5}$$

where μ_c is the mean and Sc is the standard deviation. A normal $\Delta\sigma$ variation can be represented by;

$$\Delta\sigma = \text{Gau}\,(\mu_{\Delta\sigma}, S_{\Delta\sigma}) \tag{6}$$

where $\mu_{\Delta\sigma}$ represenst the mean and $S_{\Delta\sigma}$ is the standard deviation. The a_i and a_d distributions can also be assumed to be log-normal.

$$\text{or} \quad \log a = \text{Gau}\,(\mu_a, S_a) \tag{7}$$

where μ_a represents the mean and S_a is the standard deviation. The number of cycles (N_d) required to propagate a_i to a_d can be represented by;

$$N_d = f\,(C, \Delta\sigma, a_i, a_d) \tag{8}$$

Equation (5) to (7) can be combined with equation (3) to generate an N_d distribution and a SII value can be picked from this N_d distribution at an appropriate failure probability, for example, 0.1 %F. It can be suggested that with the central limit theorem, a large N_d data base may follow a log- normal distribution if a random variable does not dominate the product of the variables in equation (8) [Ref. 1].

$$f(N_d) = \frac{1}{\sqrt{2\pi}\zeta N_d} \exp\left[-\frac{1}{2}\left(\frac{\ln N_d - \lambda_1}{\zeta}\right)^2\right] \tag{9}$$

λ_1 and ζ are related to the mean and standard deviation of the variate.

DFM or PFM approaches were used to calculate N_d where equations (3) and (8) clearly indicate that N_d predictions were strongly influenced by the crack length values used for a_i and a_d. A single (worst case) a_d value is a group of components which use the best estimates of service loads and material properties. In contrast, the a_i value chosen for calculating N_d through equation (3) and (8) will

depend upon the detection and sizing capabilities of the NDI technique which is used to inspect the components. A number of NDI techniques should be quantified in terms of crack detection capabilities (sensitivity) and reliability (probability of detection) in order to select the most suitable NDI technique for implementing the DTLP procedures for a given set of components. A way of assessing the suitability of a given NDI technique can be through a statistically valid demonstration programme.

CHAPTER III

STATISTICAL ANALYSIS OF NDI DATA

The experimented data can be grouped into three categories which can be used to evaluate the reliability of NDI techniques [Ref. 5];

Category 1 - NDI Sensitivity at One Crack Length

It is demonstrated that a NDI system is able to detect at least a given percentage of cracks at a certain length with a specified confidence limit. For example, this approach could be used to show that there is 95% confidence that at least 90% of all cracks of length X mm will be detected. These experiments have limited use as the information provided is only for the crack length inspection.

Category 2 - Estimation of POD with One Observation Per Crack

In this category, several components including a range of crack lengths are inspected once and then results are used to determine the POD as a function of crack length with confidence bounds. The crack lengths are grouped into intervals of crack length because there are not enough number of cracks of the same length. It is assumed that all cracks in specified interval have the same POD value.

Category 3 - Estimation of the POD with Multiple Observations Per Crack

An experiment performed by the U.S. Air Force, known as the "How Cracks Will Travel" programme was assisted by a large NDI reliability programme where sections of aircraft air frame were transported to depots and inspected for cracks by using various NDI systems. This method of collecting data provided an estimate of a POD for each individual crack. The most important factor of this experiment demonstrated that not all cracks of the same length have the same POD [Ref. 23].

3.1 Probability of Detection Curves (POD)

Results of the NDI techniques used in this study consisted of three possibilities. A 'Hit' is when a crack exists and NDI technique identifies the crack. A 'Miss' is when a crack exists but the NDI technique does not detect it. A 'Falls Call' refers to the case when a crack does not exist but the NDI method incorrectly indicates a crack. Hit or Miss rates are defined as the number of cracks detected or missed over the total cracks present. Falls Call rate is the ratio of Falls Calls to the total number of crack-free sites. The inspection results were statistically evaluated considering the probability of detection (POD) as a function of crack size and the 95% lower confidence bound on POD curve.

For the output of POD analysis, values of 1 or 0 are given to 'Hit' and 'Miss' respectively. For 'Hit/Miss' type data is generated on the basis of one inspection per crack (Category 2 type).

The existance of false calls in inspection data can bias a POD curve, because when false calls are high, a portion of the detected cracks are likely to be false indications at crack sites. Within such cases, the inspection results are better to be called Probability of Indication (POI) rather than Probability of Detection (POD), as the amount of false calls should be considered. The analysis described in Ref. 3 has been defined as POI (a) as the probability of obtaining an indication of a crack at crack length a, POD (a) probability of correctly detecting a crack at crack length a, and p as the probability of false indication or the false call rate. It can be assumed that p is independent of crack size. The relationship between these variables can be indicated as the following example;

$$\text{POI (a)} = p + \text{POD (a)} - \text{Prob (false call and detection)} \tag{10}$$

which states that the POI is given by the sum of the false calls p and the correct indications POD, excluding the overlap. This equation can be expanded to:

$$\text{POI (a)} = p + (1-p)\,\text{POD (a)}$$

or

$$\text{POD(a)} = \frac{\text{POI(a)} - p}{1-p} \tag{11}$$

Ways for finding POD (a) assist in providing results for POI (a), for which a limiting falls call rate is inspected. It can be seen that a small false call rate POI (a) shall be a good representation of the POD (a). Reference 3 suggests a maximum false call rate of 5% (or p0.05) to help ensure an accurate modelling of the true POD. However, if the available inspection data is not sufficient to determine

the POD (a) curve and if this has affected our POD (a) data, then we assume that a false call rate is not affected in this study. Therefore, it can be said that only a POD curve is represented.

The binomial distribution has traditionally been used for the probability of detection curves and to specify the confidence bound for POD values. The POD is defined as the ratio of cracks which shall be detected by the NDI technique compared to the total number of cracks present in the same size range. For Categories 1 and 2, the distribution mentioned is considered better to fit the observed data compared to that of other distributions such as the Chi-square, normal and Poisson distributions [Ref. 24]. The disadvantage of the binomial distribution includes the confidence bounds to be significantly influenced by the method of assigned cracks to an interval and the number of cracks contained in each intervals. Also Category 3, type data have demonstrated that cracks of the same length may consist of different POD values [Ref. 13].

Therefore, the binomial distribution is not suitable for representing the POD values since a specific crack length repeatidly consists of the same probability of detection.

Berens an Hovey (Ref. 5) have examined a number of distributions including Weilbull, Probit, Logodds-linear scale, and Log-logistics in order to determine the best for the analysis of the POD data. With the performance of an appropriate transformation compared to that of the detection probabilities and crack lengths, a linear regression analysis was carried out to determine the consistency of each distribution. Consistency was defined by Berens and Hovey as the failure to reject the hypothesis at the 0.1 level of significance [Ref. 5]. It was proven that no

other distribution modelled the POD date as consistenly as the log-logistic distribution.

The functional form of the log-logistic distribution is as follows:

$$P_i = \frac{\exp(\beta_0 + \beta_1 \ln a_i)}{1 + \exp(\beta_0 + \beta_1 \ln a_i)} \qquad (12)$$

where;

P_i = Probability of detection

a_i = Crack length

βo = Location parameter

$\beta 1$ = Slope parameter

$\dot{I}$ = 1 to; where n = Total number of crack size intervals

In order to determine the POD as a function of crack length for NDI data of Category 3 type, the a_i, P_i data pairs can be put directly into transformations which are required by the analysis. However, for Category 2, the cracks need to be grouped into intervals of crack length. The grouping must be done according to the proportion of detection, assigned to a single crack length representative of the interval. Berens and Hovey (Ref. 5), have suggested that the centre of each interval would be more representative of the detection probability than the maximum crack length in that interval.

For linear regression, analysis are given n pairs of ai, Pi data points and the log-logistics transformations can be performed by [Ref. 5].

$$Y_i = \alpha + \beta X_i \quad (13)$$

where $$Y_i = \ln (P_i / (1-P_i)) \quad (14)$$

and $$X_i = \ln (a_i) \quad (15)$$

α and β are the intercept and slope which are found from the linear regression analysis. In the cases where no cracks or all cracks are found, values for Pi are defined to be $^{1}/_{(n+1)}$ $^{n}/_{(n+1)}$, respectively.

The log-logistic curve represents the mean POD for a crack length. Standard statistical distributions such as F-distribution, student-t distribution and the normal distribution can be used to find the confidence bounds on the linear regression line based on the log-logistic curve can be then transformed back to the POD curve.

3.2 The 90% POD / 95% Confidence Curve

For the normal and the stundent-t distributions, the 95% confidence bounds were closer to the mean POD line and the distribution was detected as normal. The 95% confidence bound in the case of the normal distribution was determined by [Ref. 4].

$$\text{POD 95\% Confidence} = \text{POD mean} \pm 1.96\ S_{y/x} \quad (16)$$

Where 1.96 is the normal standard variable for a confidence interval of 0.95 and Sy/x is the conditional standard variable. This assumption lead to a lower

bound 95% confidence curve which also takes a log-logistic form with the same slope as the mean POD line but with a different intercept value in equation 12.

CHAPTER IV

EXPERIMENTAL WORK

4. Material and Methods

4.1 Experimental Material

The test components used in this study were service-expired compressor discs obtained from an J85-CAN40 engine. The specially chosen compressor discs remained in service for beyond the safe-life limit due to the logistic problems with the replacement of parts. The discs are fabricated from precipitated hardened martensitic stainless steel (AM355). Two discs are being used and each disc has 40 bolt holes of 4.8 mm (0.188") diameter. Shape and a cross section of the disc are given in Figure 2 and 3. These components are subjected to low cycle fatigue and as a result, cracks at the bolt holes were present in all of the retired parts (Ref. 10). Therefore, only the bolt holes were inspected.

The precipitation-hardenable stainless steel [Ref. 11 and 15] was developed in the 1940's. This was when the first alloy of this type, stainless W, was introduced. There have been three types of precipitation-hardenable grades developed; austenitic, semi austenitic and martensitic. The austenitic, semi austenitic and martensitic are all hardened by using a final aging treatment that precipitates very fine second-phase particles from a supersatured solid solution. Precipitation places strain on the lattice which assists with the strengthening. Maximum

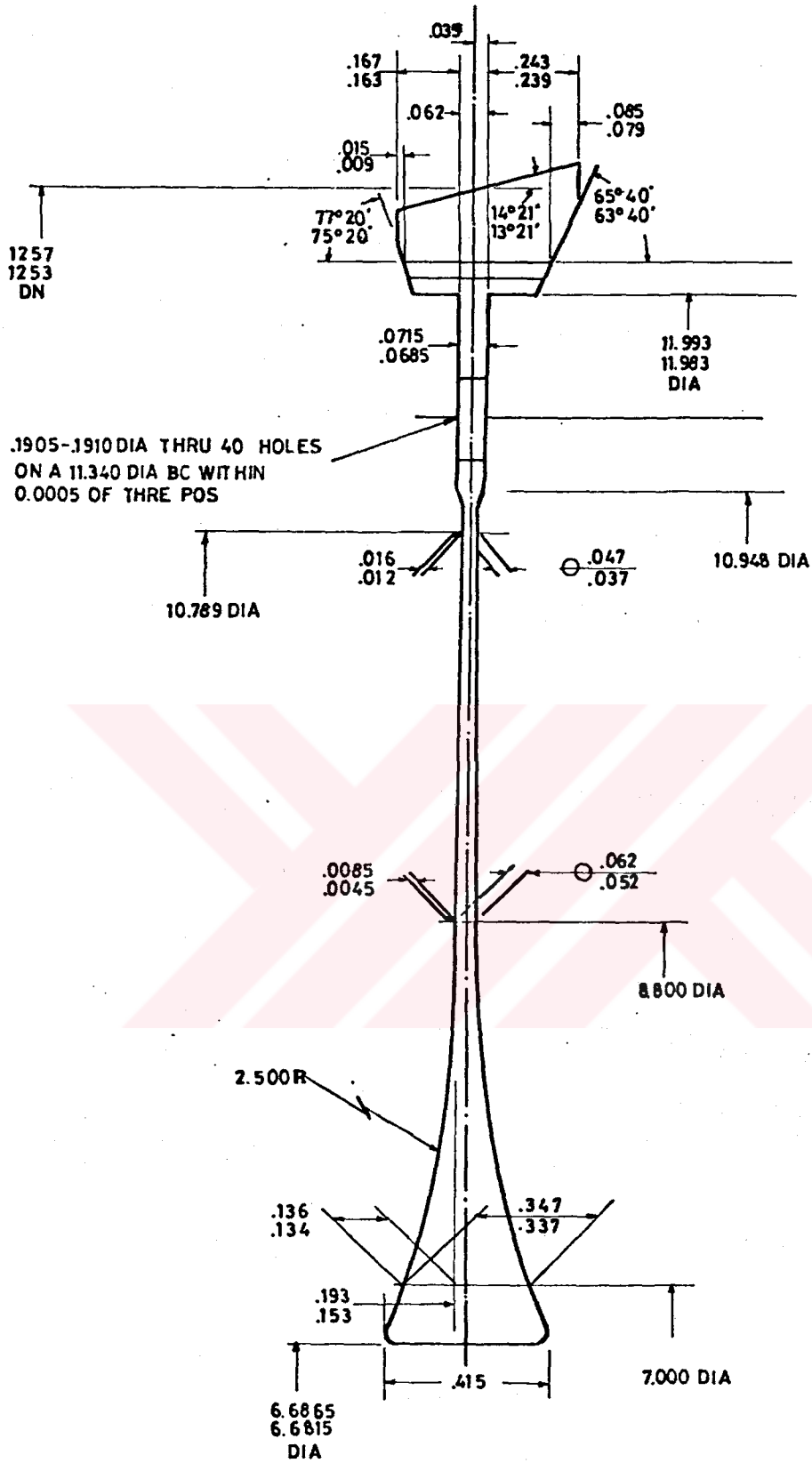

Figure 3. Cross Section of Compressor Discs

4.2 Experimental Methods

4.2.1 Liquid Penetrant Inspection Method (LPI)

Regardless of the type of penetrant used, penetrant inspection requires at least five essential steps as follows;

a) Surface Preparation

In order to allow the frequent flow of liquid to penetrate, parts should be free from foreign matter. Surfaces of the material must be free from oxide particles, scale, rust, grease traces, etc. Also, dry strains should not be visible as the fluorescent penetrants are likely to give false indications. The most suitable cleaning process has to be established according to the type of surface contamination; e.g for degreasing of grease matter Vapour of trichloroethylene, with sodium hydroxide can be used. In this study, bath of NaOH was used for cleaning the surface of the compressor discs at room temperature.

b) Application of Liquid Penetrant

After work piece has been cleaned, penetrant is applied in a suitable way to form a continuous and a uniform film of penetrant over the surface of the work piece. Ability to form a uniform film of penetrant over the surface depends on surface properties of penetrant and the surface of the workpiece. When the penetrant contacts with a solid surface, adhesive forces and cohesive forces take place between the solid surface and the molecules of the liquid. These forces determine the contact angle, θ, between the liquid and the surface. To obtain a good film of penetrant, the contact angle, θ, must be smaller than 90°. This is known as 'Wetting'. The wetting

forms the basic principle of liquid penetrant technique. This film should remain enough time on the surface to allow maximum penetration of the penetrant into surface openings that are present. The contact time can be from 2 minutes to 30 minutes for smaller cracks. The contact time depends on the type of penetrant i.e. viscosity and surface tension of a penetrant.

The ability to penetration increases with increasing temperature. When the temperature increases, the viscosity of penetrant will decrease so the penetration will increase. Generally the process is carried out at room temperature except special cases, this is sufficient to ensure good penetration. Thus, for this study, the penetrant was applied to compressor discs at room temperature.

Because of the differences among applications for liquid penetrant inspection, it has been necessary to refine and develop the two types of penetrants i.e. type 1, fluorescent and type 2, visible, into four basic methods. These methods are classified as;

1. Water-Washable (Method A)
2. Postemulsifiable lipophilic (Method B)
3. Solvent removal (Method C)
4. Postemulsifiable hydrophilic (Method D)

In this study, fluorescent liquid penetrant was used (commercially known as Beta NT sprey) and water washable method was applied in the NDI laboratory. This method and fluorescent type penetrant was used because it offered greater sensitivity due to the indication of defects appears brighter, through fluorescence on dark surface. So the defects can be seen easily.

c) Removal of Excess Penetrant

Once the contact time has been reached the excess penetrant was removed from the surface. The removal method is determined by the type of penetrant used. Some penetrants can be washed away with water whereas others require the use of emulsifier (lipophilic or hydrophilic) or solvent/removers. Uniform removal of excess surface penetrant is necessary for effective inspection. In this study water was used for removal of excess penetrant from the surface of the compressor discs.

d) Development

Developer is used to assist natural draw of the penetrant out of surface from inside the cracks and to spread it at the edges in order to enhance the penetrant indication and also to increase the brightness intensity. Developing reduces inspection time so it is desirable to use in all applications.

The developers may be dry or wet. Dry developers are used for fluorescent penetrant but should not be used with visible type penetrant because they do not produce a good contrast coating on the surface of the work piece. Because it is non fluorescent the cracks are easily detected under fluorescent light.

In this study, dry powder developer which is called BT 70 (Beta) commercially, was applied to compressor discs after drying. By applying the developer the uniform thin powder film was formed on the surface of the discs. The

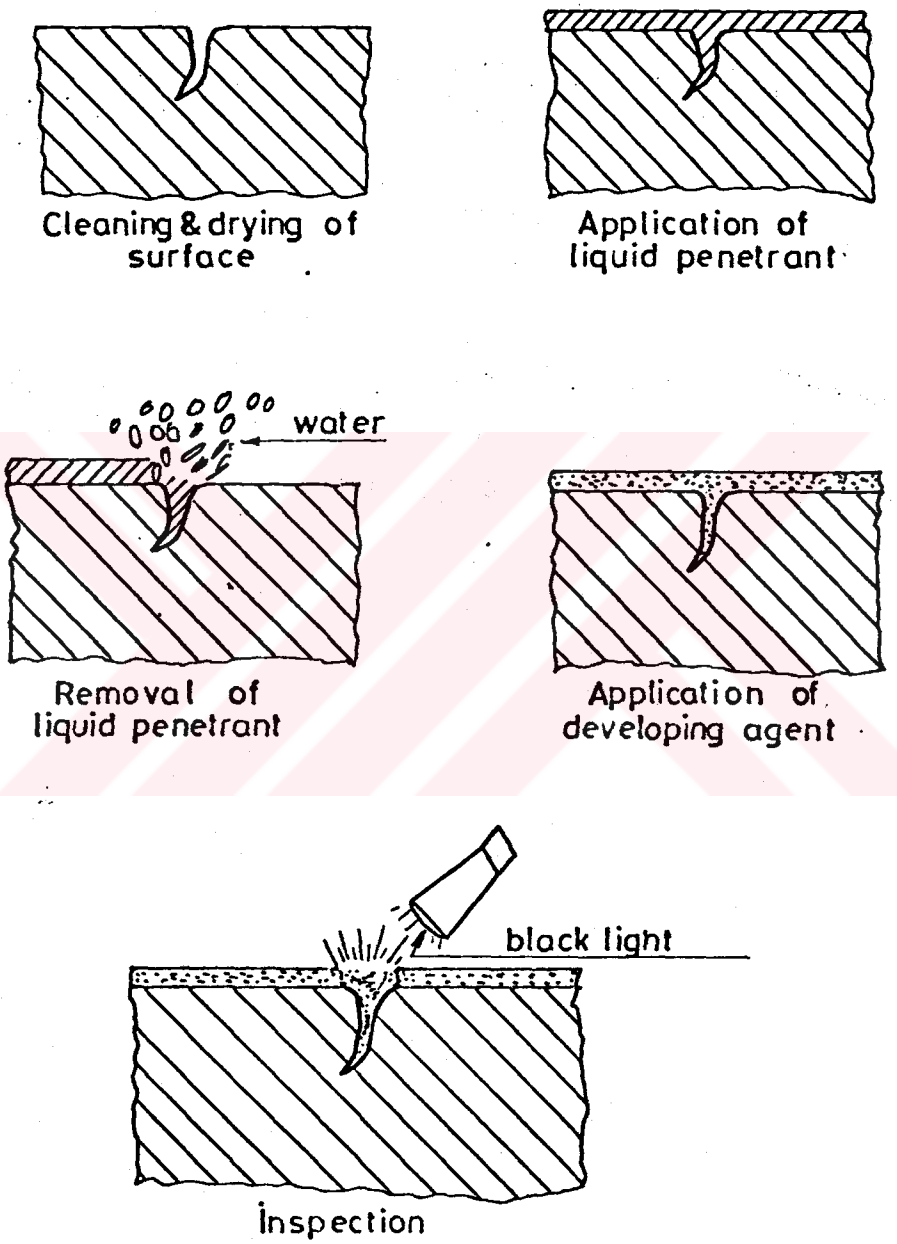

Figure 4. Essential Operations For Liquid Penetrant Inspection

penetrant heat was present on the cracks absorbed. The developer sucked the penetrant and dyed the powder to indicate the cracks.

e) Inspection

The surface is thoroughly examined for indications of penetrant bleeding on the reverse of the surface opening. This examination was performed in a suitable inspection environment with relevant equipment.

Visible penetrant inspection is performed in clear white light. When fluorescent penetrant was used inspecton was performed in an extremely darkened room using black light (ultraviolet).

4.2.2 Eddy Current Inspection

Basic Principles

Eddy Current inspection is based on the principles of electromagnetic induction and is mainly performed with the aid of surface probes and an impendance measuring device. An oscilator sends into the probe coil a high frequency alternating signal.

When a flat metalic test block comes into contact with the probe, a part of the magnetic flux produced by the coil will enter the metallic material and generate induced currents into it. These induced currents are called Eddy Currents.

These currents are circular, paralel to the surface and their direction is given by the Lenz Law. The magnetic field produced by the Eddy Currents is in opposition to the magnetic field generated by the probe. Their magnitude and timing (or phase) depends on;

* Electrical properties of the part.
* The electromagnetic fields established by currents flowing within the part.

The flow of Eddy Currents in the part depends on;

* The electrical characteristics of the part.
* The presence or absence of the flaws or other discontinuties in the part.
* The total electromagnetic field within the part.

Eddy Currents behave identically to other currents. Eddy Currents meet inside the metallic test block, ohmic resistance and self inductance.

The impendance depends on many factors:

* The material conductivity
* The material magnetic permeability μ
* The distance between probe and material (lift-off)
* The geometry and magnetic characteristics of the probe
* The presence of defects with the material
* The signal frequency = $w/2\pi$

The relation between impedance and these different factors is the basis of Eddy Current.

There is a relation between the depth of penetration (skin depth) and the frequency, this relation has been defined by Lord Rayleigh using the Maxwell Theory. Figure 5 shows this relation and it gives the depth of penetration of eddy currents for different materials.

Figure 5 is very useful, it helps the NDI technicians to know if the selected frequency of his equpment is compatible with the depth or location of the defect.

In this study, in order to inspect the discs using eddy current, NDT technicians has assisted to set up the experiment. Equipment used in 2.832/FOERSTED and its rotating probe. The diameter of rotating probe was 4.7mm. The instrument setting of Eddy Current Inspection was as below:

Frequency = 500 kHz
Filter = HP5
Preamplifier = -6
Current + Ddive = 2
Y Expansion Y/X = 6
Phase = 23
Sensitivity = 32 dB

Crack was identified by the signal displayed on the screen of Eddy Current Equipments.

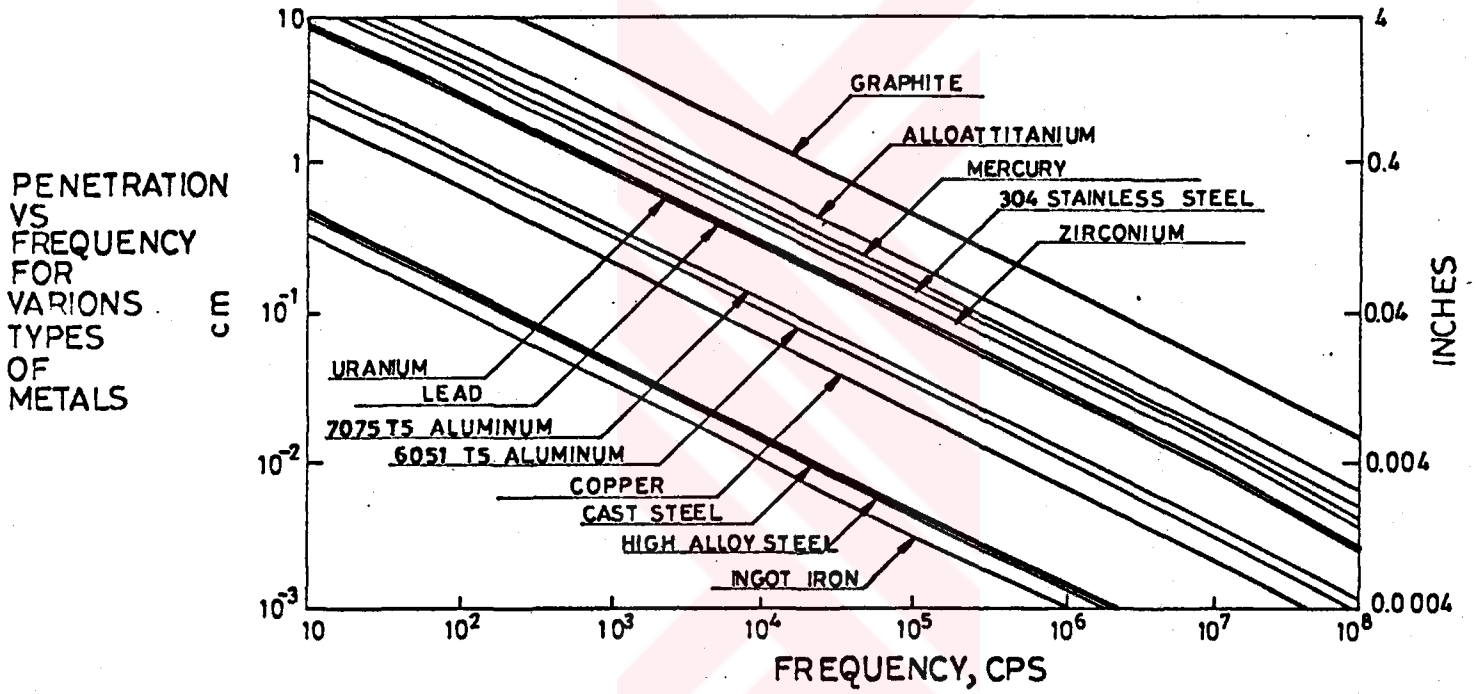

Figure 5. Standard Depths of Penetration as a Function of Frequencies Used in Eddy Current Inspection for Several Metals of Various Electrical Conductivities

4.3 Optical Microscope Inspection

An optical microscope was used to inspect the components for surface breaking cracks. The surface finish, the crack opening and the crack surface length are important factors to supply success of optical microscope inspection. The geometry of test components made it difficult to examine the bore surface of the holes.

4.4 Destructive Crack Verification

After the completion of all NDI, the existance of cracks in the bolt holes was verified by Destructive Testing. The crack verification process is schematically illustrated in Figure 6. First the outer part and then the inner part of the compressor discs were cut out by using the plasma cutting machine, then approximately 2 cm x 3 cm samples were cut from the region surrounding each bolt hole by using the shear cutting machine. Each sample was then sectioned into two pieces along the diameter of the bolt hole. In the inward piece (the large seciton), a notch was introduced in the side opposite to the bolt hole and the sample was then pried open by closing the notch in a vice. After pry opening, the fracture surfaces were examined under an optical or a scanning electron microscope (SEM) as required, depending on the crack size. Under the microscope, the service-induced low cycle fatigue (LCF) cracks were easily recognized from the rupture failure due to their smooth and oxidized surfaces and the crack size was measured. The specimens that did not reviel a crack on the fracture surfaces were examined again on the bolt hole surface to be certain that a crack was not missed during the pry opening operation.

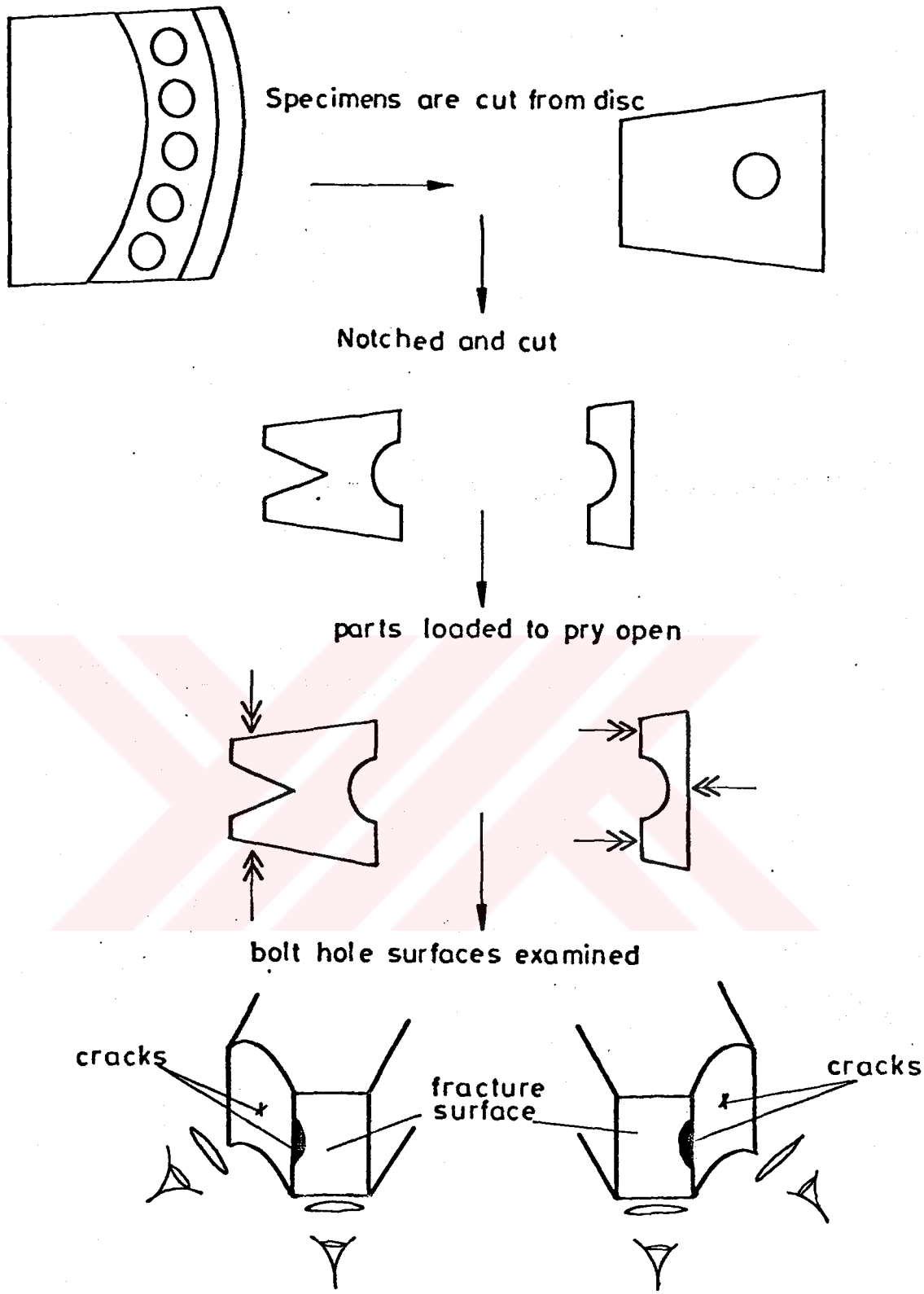

Figure 6. Schematic Illustration of Sectioning, Pry Opening and Examination of Bolt Hole Specimens.

4.5 SEM Examination of Compressor Discs

After the non destructive inspections and optical microscope inspections were completed, the material surrounding all bolt hole areas were cut out into coupons as shown in Figure 6.

Crack lengths and geometries are measured by a Scanning Electron Microsopy (SEM). As it has been mentioned previously; the compressor discs created from AM 355, a precipitating hardened martensitic steel, each disc contains forty tie bolt holes which were used to assemble the compressor section. SEM examination was shown that low cycle fatigue cracks initiate at the bolt hole and grow radially towards the bore of disc. On several occassions the cracks have been found to grow radially outward.

CHAPTER V

RESULTS

5.1 Inspection Data

The inspection results have been outlined in Table 1 and 2. The results have displayed for the Liquid Penetrant Inspection Method and the Eddy Current Inspection with the indications of "1" for a hit, "0" for a miss and "f" for a false call. Results are based on the outcome of destructive tests which are represented along with the crack size (maximum length and total area), the number of cracks in each bolt hole and the location of the largest crack.

5.2 Crack Shapes

Tests and examinations of the fracture surface displayed numerous cracks which were visible near the edges of the holes and cracks had also formed on the corners of the material tested. Often, it was detected that the cracks had grown radially inward towards the center of the component. Several cracks which did not touch the top or bottom surfaces were present and these were termed as middle cracks. Cracks which touched both surfaces were referred to as through cracks. Examples of different crack types are provided in Figures 7, 8, 9 and 10. The amount of cracks present were as follows; corner cracks (17), middle cracks (11) and through cracks (5).

Table 1. Inspection Data

		Hole #	Depth (mm)	Opening (mm)	Area (mm^2)	LPI	Eddy Current
D I S C 1		9	1.4 0.1	1.5 0.3	1.8 0.07	0 0	1* 1
		12 14 23 25	1.6 0.26 1.4 0.22	1.7 0.33 1.4 0.38	2.4 0.07 1.5 0.06	1 0 0 0	1 0 1 0
		26	0.45	0.49 0.23	0.18	0 0	0* 0
		27 28	0.2 0.1	0.2 0.08	0.03 0.006	0 0	0 1
		30					F
		31					F
		32	0.18 0.09 0.04	0.3 0.12 0.10	0.04 0.005 0.003	0 0 0	1* 1 1
		33 34 40	 1.5 0.25	 1.6 0.52	 1.8 0.1	 0 0	F 1 0
D I S C 2		1	1.0 0.02 0.25	1.2 0.04 0.45	1.0 0.0008 0.1	0 0 0	1* 1 1
		2	0.28 0.04	0.31 0.04	0.06 0.02	0 0	0* 0
		3 6 15	0.3 0.06 0.26	0.95 0.09 0.46	0.14 0.006 0.09	0 0 0	0 0 0
		16	0.08 0.025 0.03 0.09 0.05 0.04	0.2 0.04 0.07 0.11 0.09 0.05	0.01 0.0008 0.0015 0.015 0.004 0.004	0 0 0 0 0 0	0 0 0 0* 0 0
		17	0.33 0.21	0.71 0.32	0.16 0.05	0 0	0* 0
		18	0.44 0.04 0.02 0.03 0.04	0.41 0.06 0.04 0.025 0.09	0.14 0.003 0.0004 0.001 0.003	0 0 0 0 0	1* 1 1 1 1

Table 1. (Cont'd)

		Hole #	Depth (mm)	Opening (mm)	Area (mm^2)	LPI	Eddy Current
		19	0.17 0.07 0.043	0.35 0.09 0.025	0.046 0.004 0.003	0 0 0	0* 0 0
		20 23 24 25 27 31	0.055 0.55 0.15 0.05 0.07	0.085 0.55 0.17 0.07 0.11	0.004 0.24 0.017 0.002 0.006	0 0 F 0 0 0	0 0 0 0 0
		33	1.28 0.05	1.28 0.11	1.29 0.04	0 0	1* 1
		34	2.0	1.7	3.3	1	1
		35	1.3 0.88	1.26 0.7	1.29 0.53	1 1	1* 1
		36	1.7 1.25	1.5 0.92	2.0 0.9	0 0	1* 1
		37	2.2	1.7	3.9	1	1
		38	1.25 1.05 ?	1.50 0.52 0.15	1.7 ? ?	1 1 1	1* 1 1
		39 40	1.58 1.3	1.7 1.7	2.2 1.6	1 0	1 1

Table 2. Inspection Results

	No. of Crack	Hole #	Depth (mm)	Opening (mm)	Area (mm^2)	LPI	Eddy Current
	1	9	1.4	1.5	1.8	0	1
D	2	12	1.6	1.7	2.4	1	1
I	3	14	0.26	0.33	0.07	0	0
S	4	23	1.4	1.4	1.5	0	1
C	5	25	0.22	0.38	0.06	0	0
	6	26	0.45	0.49	0.18	0	0
1	7	27	0.2	0.2	0.03	0	0
	8	28	0.1	0.08	0.006	0	1
		30					F
		31					F
	9	32	0.18	0.3	0.04	0	1
		33					F
	10	34	1.5	1.6	1.8	0	1
	11	40	0.25	0.52	0.1	0	0
	12	1	1.0	1.2	1.0	0	1
	13	2	0.28	0.31	0.06	0	0
	14	3	0.3	0.95	0.14	0	0
D	15	6	0.06	0.09	0.006	0	0
I	16	15	0.26	0.46	0.09	0	0
S	17	16	0.09	0.11	0.015	0	0
C	18	17	0.33	0.71	0.16	0	0
	19	18	0.44	0.41	0.14	0	1
2	20	19	0.17	0.35	0.041	0	0
	21	20	0.055	0.085	0.004	0	0
	22	23	0.55	0.55	0.24	0	0
		24				F	
	23	25	0.15	0.17	0.017	0	0
	24	27	0.05	0.07	0.002	0	0
	25	31	0.07	0.11	0.006	0	0
	26	33	1.28	1.28	1.29	0	1
	27	34	2.0	1.7	3.3	1	1
	28	35	1.3	1.26	1.29	1	1
	29	36	1.7	1.5	2.0	0	1
	30	37	2.2	1.7	3.9	1	1
	31	38	1.25	1.5	1.7	1	1
	32	39	1.58	1.7	2.2	1	1
	33	40	1.3	1.7	1.6	0	1

Figure 7. Corner Crack

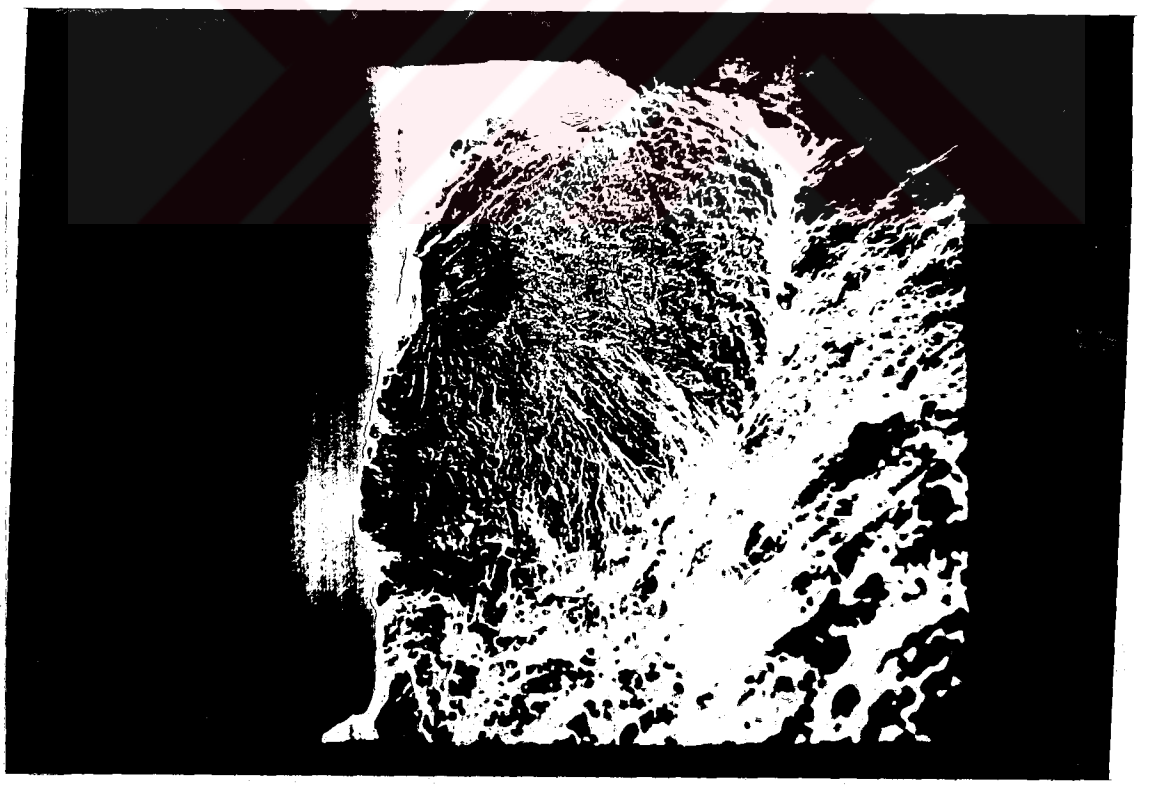

Figure 8. Middle Crack

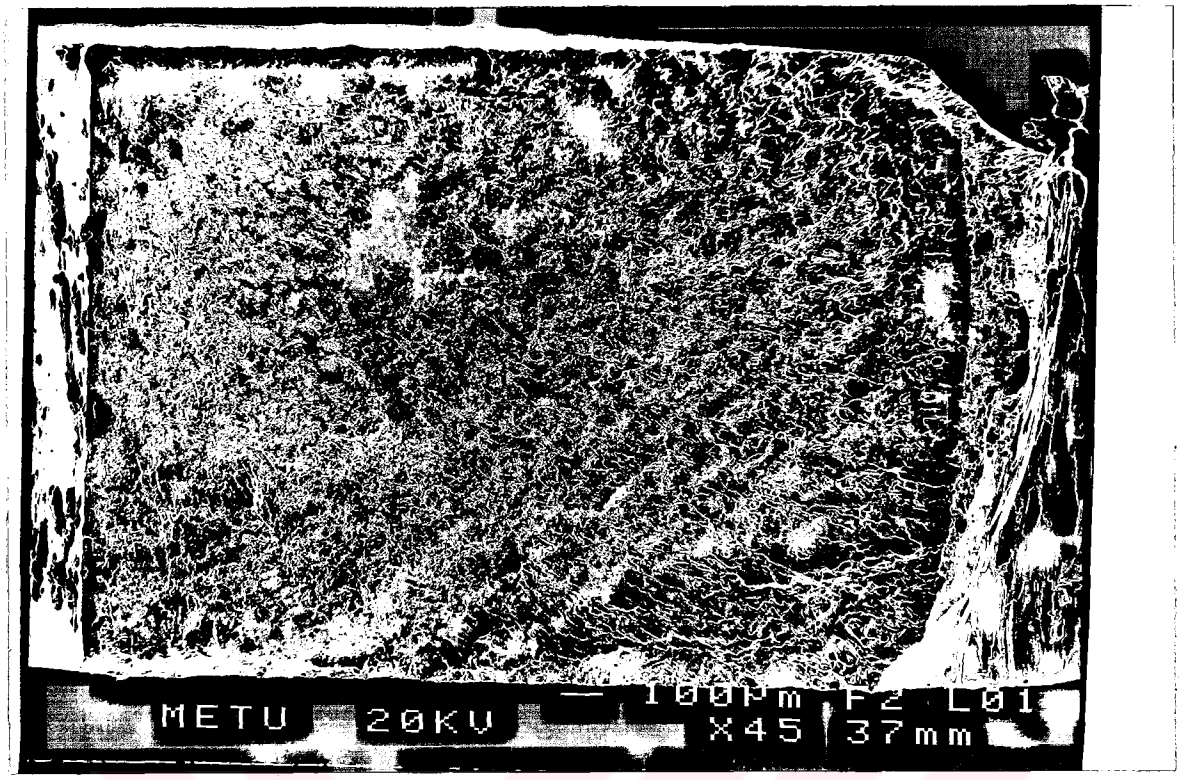

Figure 9. Through Crack

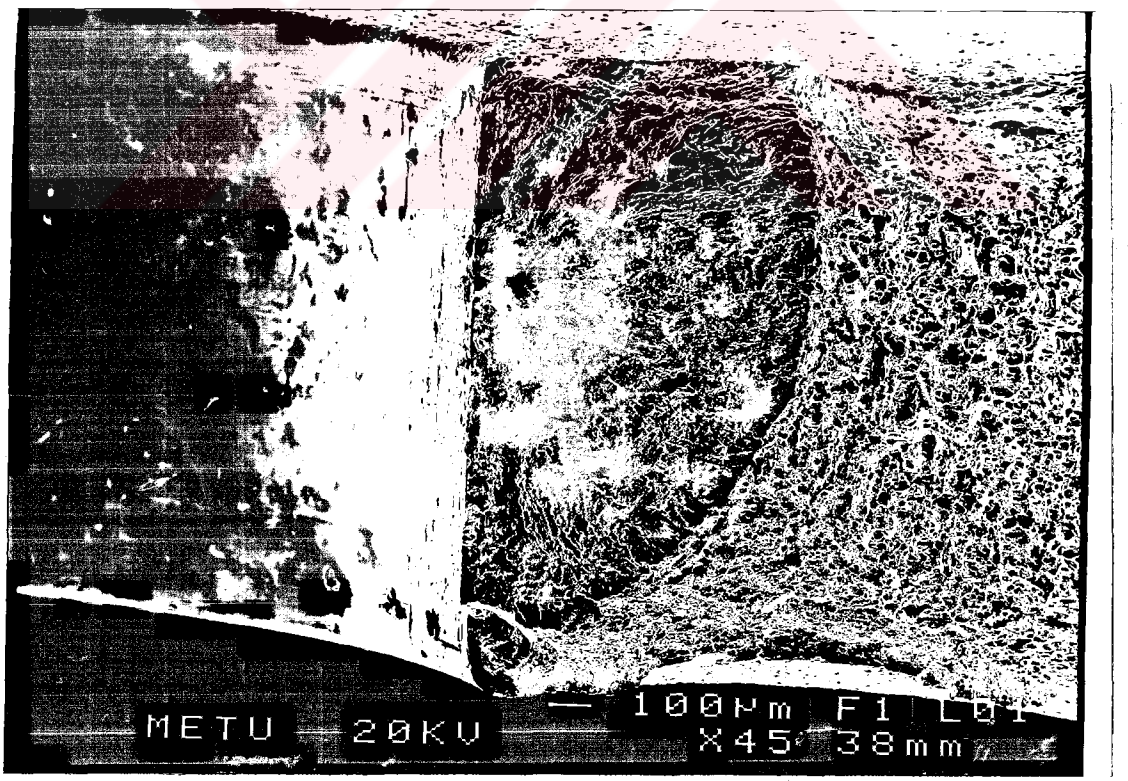

Figure 10. Multiple Crack

A numerous number of holes were seen to have a single crack and a total of 13 had holes with multiple cracks. Some cracks didnot occur along the radii of the discs for which many of these were initiated at what appeared to be voids or inclusions in the material and were often accompained by longer cracks on the radii. Several internal cracks and outward propagating cracks were also seen.

The location of the cracks is an important indication as the shape of the cracks varied depending on their location. Middle cracks were mostly semi-ellipse and through cracks were close to rectangular shape. A combination of the above shapes were often seen in the cases of multiple cracks. Where failure did not occur through a crack, the bore surface of the bolt hole was examined and if a crack was found, the crack length of the surface was measured.

5.3 Histograms

Since the experimental data from this investigation is of Category 2 type (one inspection per crack), the crack length was grouped into intervals in order to obtain a significant number of cracks to determine realistic POD values. The best compromise between the number of intervals and the number of cracks in each interval was achieved at an interval of 0.4 mm.

Figures 11 and 12 display histograms of the number of cracks detected, the total number of cracks and the number of cracks missed as a function of the crack length interval for Liquid Penetrant Inspection and Eddy Current Inspection.

Table 3 contains a summary of the test results which compare the performance of the Liquid Penetrant Inspection and Eddy Current Inspection.

The histograms shown in Figures 11 and 12 were used to obtain the observed POD data points by calculating the ratio of the number of cracks detected in each interval to the total number of cracks in that interval. These points were then used in the linear regression analysis (Equation 12 to 15) to obtain log-logistic POD curve.

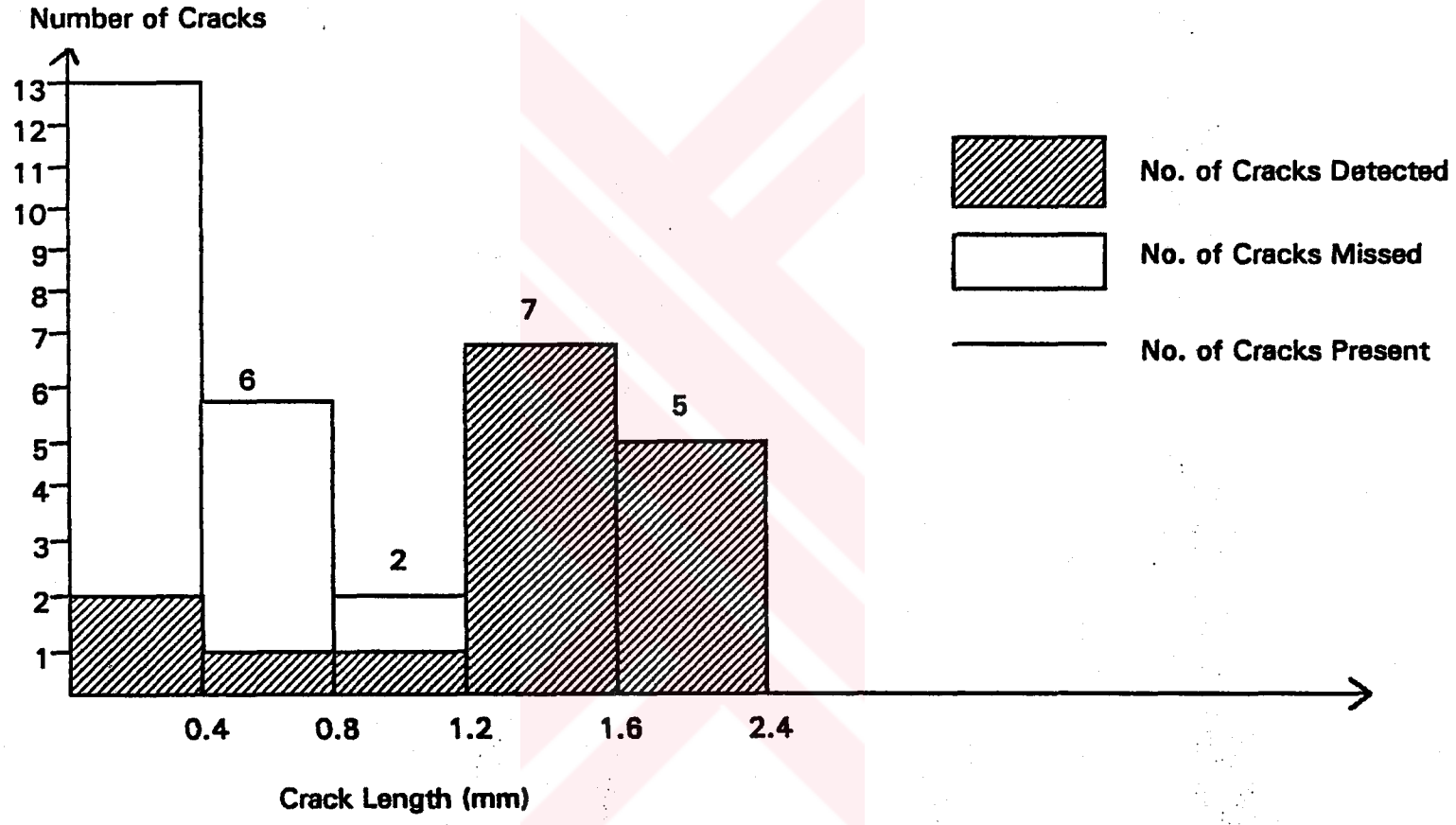

Figure 11. Histogram of Eddy Current Inspection

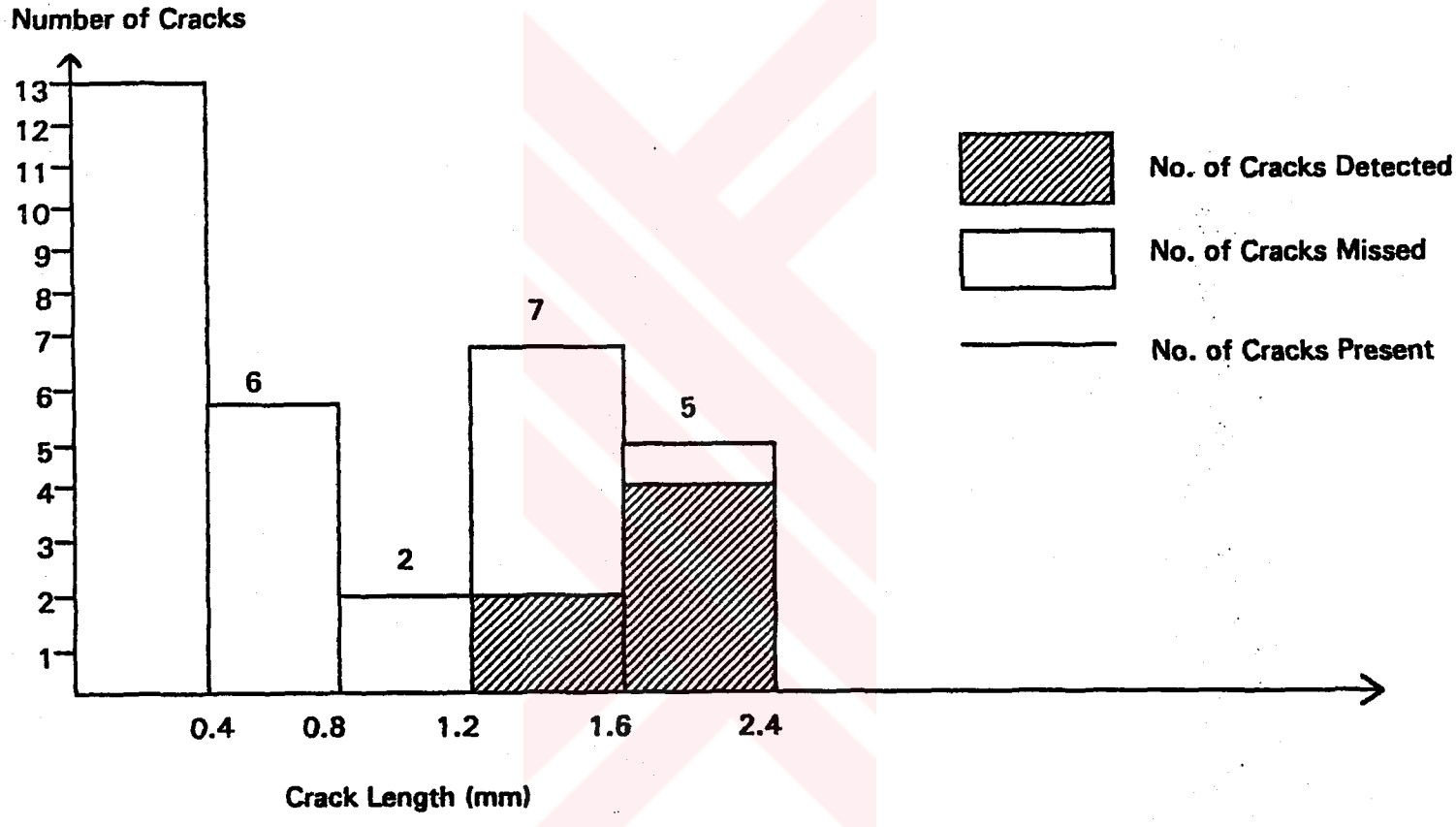

Figure 12. Histogram of LPI Method

Table 3. Summary of Results for NDI Techniques

NDI Techniques	No. of Cracks Detected		No. of Cracks Missed		No. of False Calls		Smallest Crack Detected (mm)	Largest Crack Missed (mm)	90% POD mean (mm)	90% POD confidence limit (mm)
	Total	%	Total	%	Total	%				
Eddy Current	16	48.5	17	51.5	3	9.1	0.08	0.95	1.27	1.72
Liq. Penetrant	6	18.2	27	81.8	1	3.0	1.26	1.7		

CHAPTER VI

DISCUSSION

80 bolt holes were examined by an optical microscope and later by SEM. In the performance table of LPI and Eddy Current Inspection Methods resulted in 16 detection (48.5%), 17 misses (51.5%) and 3 falls calls (9.1%). The largest crack which was missed by the Eddy Current was 0.95 mm in length. The liquid penetrant inspection method resulted in 6 detections (18.2%), 27 misses (81.8%) and 1 false call (3%). The largest crack missed by the liquid penetrant inspection was 1.7 mm in length.

In the POD curve of Eddy Current Inspection method, the intercept of 90% POD with mean POD line was 1.27 mm in length and the dectectable at 90% POD with 95% confidence for the eddy current technique was 1.72 mm obtained from Figure 13.

As mentioned in the previous chapters of my thesis, the 90% POD at 95% confidence limit was established for damage tolerance applications for aircraft airframe structures where most of the critical components were not really accessible. The gas turbine engine was disassembled in order to inspect the different components, each component was inspected as many times as was seen necessary to obtain the results required. Therefore, it is now suggested that the intercept point of the 90% POD with the mean POD line may be a more realistic criteria for choosing

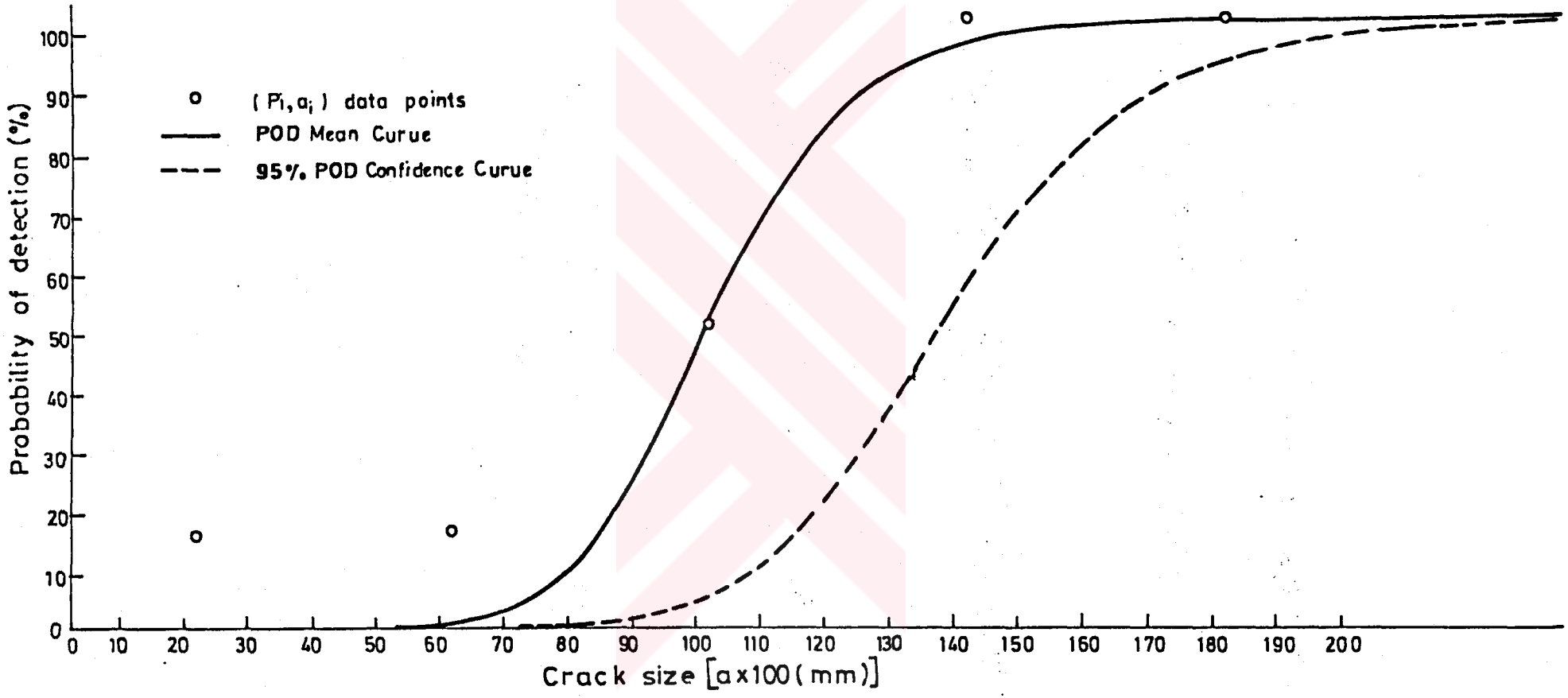

Figure 13. POD Curve of Eddy Current Inspection

the best NDI technique for implementing the damage tolerance based maintance methods given for engine components. These limiting cracks are given in Table 3.

The POD curve of the LPI method was not drawn due to insufficient data not being distributed randomly. Therefore, the crack sizes for 90% POD and 90% POD at 95% confidence level could not be found.

As it was said before that the false call rate is high in the Manual Eddy Current Inspection (9.1%) and this value was used for calculation of POD values because of not enough number of POD data. Therefore, false call rate was ignored. If noise is present in the response signal, false indication can result if noise response from a crack free site is interpreted as being caused by a crack. False calls are undesirable for economic reason, but often there is a trade off between the false call rate and the ability to detect small cracks. False calls only marginally increase the probability of indication but not the true probability of detection. To improve the probability of detection, signal-to-noise ratio should be increased. This ration depends on mary factors including the physics of the procedure, instruments and setting employed, the test material and geometry, and the operator etc.

Traditionally, a binomial distribution has been used to specify the confidence bounds for probability of detection data because it is said to provide an optimum fit to the experimental results. But in this study binomial distribution was not used to specify the confidence bounds since the major problem with the binomial distribution in terms of the type of inspection data i.e. one observation per crack is related to the fact that the confidence bounds are significantly influenced by the number of cracks in a crack length interval. Because of this limitation log-logistic curve was the most suitable method for describing probability of detection data.

A stury similar to this study was done and the results of the study have been noted in Reference 4. In this study, 400 bolt holes were examined by several NDI techniques. The results was shown in Table 4.

Table 4 shows that the manual Eddy Current technique at a high sensitivity level detected a longer number of cracks (76% detection, 24% misses). However, the false call rate (2.4%) and largest crack 1.7 mm were relatively high and 90% mean and 90/95 POD limits were 1.25 mm and 1.75 mm respectively. In terms of detecting samall cracks (sensitvity), the Manual Eddy Current technique was superior to all other methods examined.

Table 4. Summary of Results for NDI Techniques

	No. of Cracks Detected		No. of Cracks Missed		No. of False Calls		Smallest Crack Detected	Largest Crack Missed	90% POD	90/95% POD
NDI Technique	Total	%	Total	%	Total	%	(mm)	(mm)	(mm)	(mm)
Ultrasonic Leaky Waves	167	50.2	166	49.8	2	0.6	0.17	1.48	1.85	2.90
Eddy Current 2	137	41.1	196	58.9	3	0.9	0.23	4.43	5.60	10.00
Eddy Current 5	253	76	80	24	8	2.4	0.09	1.70	1.25	1.75
LPI (45 min)	99	29.7	234	70.3	0	0	0.2	4.33	4.25	8.35
LPI (60 min)	125	37.5	208	62.5	2	0.6	0.55	3.70	3.45	6.20
LPI (30 min)	93	27.9	240	72.1	3	0.9	0.5	3.98	3.75	6.40

CHAPTER VII

CONCLUSION

Sensitvity and reliability of several NDI techniques in the detection and sizing of low cycle fatigue cracks in the bolt holes of compressor discs of J85-CAN40 engines were assesed. In this assesment, the conventional liquid penetrant and manual Eddy Current techniques have been used. The following observations were made.

The manual Eddy Current Inspection technique at a high sensitivity level helped to detect a larger number of cracks (48.3% detection and 51.5% misses). However, the rate of false calls 9.1% were relatively high. The crack lengths at 90% POD/mean and 90% POD/95% confidence were 1.27 and 1.72 mm in length respectively.

In terms of the capability of detecting small cracks (sensitivity), this technique was superior to liquid penetrant technique. In this investigation, a manual Eddy Current Technique was used enabling the probe replacement to be accomplished by hand. This method had strong influence on the reliability and sensitivity of the technique.

The liquid penetrant technique at a low sensitivity level detected a smaller number of cracks (18.2% detection 91.2% misses). A low and false call rate of 3% was noted. The largest crack missed by the LPI was 1.7 mm in length. As

mentioned previously, the POD/mean curve and 95% confidence line of LPI could not have been drawn due to the data not being suitable to draw the POD curve and that the data was not distributed randomly.

REFERENCES

[1] Ang A. , and Tang W.H. "Probability Concepts in Engineering Planning and Design, Basic Principals Vol. 1, John Wiley and Sons Inc., New York, 1975.

[2] Annis, C.G. Jr, Simms, D.L and Harris, J.A. "Concept Definition: Retirement for Cause of F100 Rotor Components", AFWAL-TR-80-4118, 1980.

[3] Annis, C.A. Jr., Petrin C., and S.I. Vukelich. "A Recommended Methodology for Quantifying NDE/NDI Based on Aircraft Engine Experience" AGARD-LS-190, 1993.

[4] Bellinger, A. Fahr, A.K. Koul, G. Gould and P. Stoute, "The Reliability and Sensitivity of NDI Techniques to Detect LFC Cracks in Fastener Bolt Holes of Compression Discs" National Research Council of Canada, NAE Report LTR-ST-1651, May 1988.

[5] Berens, A.P. and Hovey, P.W., "Statistical Methods for Estimation Crack Detection Probabilities", Probabilistic Fracture Mechanics and Fatigue Methods: Applications for Structural Design and Maintenance. ASTM STP 798, 1983.

[6] Besuner P.M. and A.S Tetelman, "Probabilistic Fracture Mechanics"; Journal of Nuclear Engineering and Design, Vol. 43., pp. 99-114, 1977.

[7] Besuner P.M., and Rau Jr., "Quantitative Decisions Relative to Structural Integrity", Trans. ASME, Vol. 102, Jan 1980. pp.56, Jan 1980.

[8] Cook, C.E. Spaeth, D.T. Hunter and R.J. Hill, "Damage Tolerant Design of Turbine Engine Discs", ASME 82-GT-311, 1982.

[9] Daub W.J., "WeibullAnalysis for Aircraft Engine Components, General Electric (J 85 Project).

[10] Fahr A., Forsyth D., Bullock M., Wallace W."NDI Techniques for Damage Tolerance Based Life Prediction of Aero-Engine Turbine Discs", Institute for Aerospace Research, LTD-ST-1961, Feb. 1994.

[11] Irvine K.J. et al. "Controlled-Transformation Stainless Steels" J. Iron Steel Inst. Vol. 92, pp. 218, July 1959.

[12] Koul A.K., Thamburaj R., Wallace W., Raizenne M.D. and Malherbe de M.C, "Practical Experience with Damage Tolerance Based Life Extension Concepts for Turbine Engine Components"; Proc. AGARD-SMP Conference on Damage Tolerance Concept for Critical Engine Components, AGARD-CP-393, San Antonio, Texas, pp. 23-1 to 23, 1985.

[13] Lewis W.H., Dodd B.D., Sprout, W.H. and Hamilton J.M. "Reliability of Non Destructive Inspections", July 1974 to December 1978, Final Report No. SAALC-MEE 76-6-38-1 US Airforce, Performing Organization Locked, Georgia Co., Controlling Office, San Antonia Air Logistics Center Kelly Airforce Base, Texas, 1978.

[14] Lewis N.H. et al., "Reliability of Nondestructive Inspections - Final Report", Report SA-ALC/MME 76-6-38-1, United States Air Force, Air Logistic Center, Kelly Air Force Base, 1978.

[15] Marcus H.L. et. al. "Precipitation in 17-7 pH Stainless Steel" Trans. ASM, Vol. 58., pp. 176, 1968.

[16] Mom, A.J.A., Evans W.J., Ten Howe, A.A. "Turbistan, a Standard Load Sequence for Aircraft Engine Discs" AGARD Specialist Meeting on Damage Tolerance Concept for Critical Engine Components. San Antonio, Texas, AGARD C.P. 393, pp. 1, April 1985.

[17] Mom, A.J.A., Raizenne, MD. "AGARD Engine Disc Cooperative Test Program" AGARD-R-766, August, 1988.

[18] Rau C.A. Jr., "The Impact of Inspection and Analysis Uncertainty on Reliability Prediction and Life Extension Stategy", DARPA/AFML Review of Progress in Quantitative NDE, San Diego, July 1978.

[19] Reed, E.J., Hunter, D.I. and Hill, R.J. "LCC Evaluation of Advanced Engine Damage Tolerance Goals for a Hot Section Disc" AIIA-83-1407.

[20] Rummel W., "Recommended Practice for a Demonstration of Nondestructive Evaulation (NDE) Reliability on Aircraft Production Parts," Mater. Eval. Vol. 40, p. 922, Aug. 1982..

[21] Scatter S.A. and Sundt C.V., " Gas Turbine Engine Disc Cylic Life Prediction". J. Aircraft, Vol. 12.(4), pp. 360, April 1975.

[22] Scatter S.A. and Hill J.T. "Design of Jet Engine Rotors for Long Life" Paper 750619 presented at SAE Air Transportation Meeting, Hartford, 1975.

[23] Thamburaj R., Koul A.K., Wallace W. and Malherber de M.C., "Life Extension Concepts for Canadian Forces Aircraft Engine Components; J85-CAN40 Compressor and Turbine Materials" National Research Council of Canada, NAE Report, LTR-ST-1585, 1986.

[24] Yee B.G.W., Chang F.H., Couchman J.C., Lemon G.H., and Packman P.F., "Assesment of NDE Reliability Data", General Dynamics, Fort Worth, Texas, July 1974, September 1976, NASA-CR-134991, Final Report, October 1976.

[25] _____,"MLT-STD-1783 Millitary Standard, Engine Structural Integrity Program (ENSIP)," Department of Defence, Washington, D.C., 20360, 30 November, 1984.

[26] _____,"Standard Practive for Fabricating and Checking Aluminum Alloy Ultrasonic Reference Block" E127, Annual Book of ASTM Standards.

[27] _____,"Standard Recommended Practice for Fabrication and Control of Steel Reference Blocks Used in Ultrasonic Inspection", E428. Annual Book of ASTM.

APPENDICES

APPENDIX A

COMPARISON OF DIFFERENT STATISTICAL DISTRIBUTIONS USED FOR CONFIDENCE BOUNDS

In order to determine the statistical distribution best suited for describing the category 2 type data presented in this study, a number of distributions can be used to calculate the 95% lower confidence bound on the log-logistic mean POD line for the different NDI techniques investigated. These distributions includes the F-distribution, normal distribution, student t-distribution and the binomial distribution.

A.1 The Normal Distribution

In the normal distribution, it is assumed that the probability of detection varies normally for a given crack length and that the variance is the same for any crack length. The 95% confidence bounds are determined using the following equation:

$$POD_{95\%} = POD_{MEAN} \pm 1.96\, S_{y/x} \qquad (A1)$$

where 1.96 is the normal standard variate for a confidence interval of 0.95 and $S_{y/x}$ is the conditional standard variance given by the following equation;

$$S_{y/x} = \left[\frac{S_{yy} - \frac{S_{xy}^2}{S_{xx}}}{n-2} \right] \quad \text{(A2)}$$

where

$$S_{yy} = \Sigma y^2 - \frac{(\Sigma y)^2}{n} \quad \text{(A3)}$$

$$S_{xx} = \Sigma x^2 - \frac{(\Sigma x)^2}{n} \quad \text{(A4)}$$

$$S_{xy} = \Sigma xy - \frac{(\Sigma x \Sigma y)}{n} \quad \text{(A5)}$$

This assumption results in a lower bound confidence line which is also a log-logistic curve with the same slope as the POD mean linear regression line but with a different intercept.

A.2 The F-distribution

The F-distribution does not assume any underlying distribution of the variation of a variable but is based on the correlation between two variables. Confidence bounds are determined by choosing the desired confidence level, 1-α (α=0.05 in this case), obtain $F_{1-\alpha}$ for two degrees of freedom (N_1, N_2) from Table A1 and then choosing the x values at which to compute points for drawing the confidence band using the following equation:

$$Y_e = \bar{Y} = b_1(x - \bar{x}) \tag{A6}$$

$$W_1 = \sqrt{2F}\ S_{y/x}\left[\frac{1}{n} + \frac{(x-\bar{x})^2}{S_{xx}}\right]^{1/2} \tag{A7}$$

where $S_{y/x}$, S_{xx} are given in Equation A2 and

$$b_1 = \frac{S_{xy}}{S_{xx}} \tag{A8}$$

where S_{xy} is given in Equation A5.

Therefore, the 1-α confidence band for the whole line is determined by:

$$Y_c - W_1 \qquad \text{(A9)}$$

A.3 The Student t-distribution

The underlying distribution of a stundent t-distribution is the normal distribution. When the number of points approaches infinity, this distribution becomes the same as the normal distribution. The confidence bounds are calculated in a similar manner to the normal distribution except that the normal standard deviate 1.96 is replaced by some t value which depends on the number of data points. The equation for determining these confidence bounds is as follows:

$$POD_{95\%} = POD_{MEAN} \pm t_{\alpha/2,n-1}\ S_{y/x} \qquad \text{(A10)}$$

where $t_{\alpha/2,n-1}$ is obtained from Table A.2 and the $S_{y/x}$ is found from Equation A2.

A.4 The Binomial Distribution

With a confidence level of 100(1-α), the lower bound on the estimate of P can be calculated as the solution, P_L, to the equation:

$$\alpha = \sum \frac{n!}{(n-i)!i!} P_L^{\,i} (1-P_L)^{n-i} \qquad \text{(A11)}$$

Solutions to this equation have been determined and are presented in Figure A.1.

There are a number of techniques which have been developed to determine the confidence bounds using the binomial distribution. The main difference between these techniques is in the manner in which the crack length intervals are created. The simplest of these methods is known as the Range Interval Method (RIM). In this method, crack length intervals are defined for equal crack lengths across the range of data. However, the lower bound confidence lines which are generated using this method can exhibit an apparent erratic behaviour due to a strong dependency on the sample size (i.e. number of crack length contained in each interval).

To eliminate this strongest dependency on sample size, Yee et al. [Ref. 24] recommended the use of the Optimized Probability Method (OPM) which provides the highest possible lower confidence bounds of all binomial distribution methods [Ref. 24]

Table A.1 Percentiles of the F-distribution $F_{.95}^{(n_1,n_2)}$

n_1 = degrees of freedom for numerator

n_2 = degrees of freedom for denominator

n_2 \ n_1	1	2	3	4	5	6	7	8	9	10	12	15	20	24	30	40	60	120	∞
1	161.4	199.5	215.7	224.6	230.2	234.0	236.8	238.9	240.5	241.9	243.9	245.9	248.0	249.1	250.1	251.1	252.2	253.3	254.3
2	18.51	19.00	19.16	19.25	19.30	19.33	19.35	19.37	19.38	19.40	19.41	19.43	19.45	19.45	19.46	19.47	19.48	19.49	19.50
3	10.13	9.55	9.28	9.12	9.01	8.94	8.89	8.85	8.81	8.79	8.74	8.70	8.66	8.64	8.62	8.59	8.57	8.55	8.53
4	7.71	6.94	6.59	6.39	6.26	6.16	6.09	6.04	6.00	5.96	5.91	5.86	5.80	5.77	5.75	5.72	5.69	5.66	5.63
5	6.61	5.79	5.41	5.19	5.05	4.95	4.88	4.82	4.77	4.74	4.68	4.62	4.56	4.53	4.50	4.46	4.43	4.40	4.36
6	5.99	5.14	4.76	4.53	4.39	4.28	4.21	4.15	4.10	4.06	4.00	3.94	3.87	3.84	3.81	3.77	3.74	3.70	3.67
7	5.59	4.74	4.35	4.12	3.97	3.87	3.79	3.73	3.68	3.64	3.57	3.51	3.44	3.41	3.38	3.34	3.30	3.27	3.23
8	5.32	4.46	4.07	3.84	3.69	3.58	3.50	3.44	3.39	3.35	3.28	3.22	3.15	3.12	3.08	3.04	3.01	2.97	2.93
9	5.12	4.26	3.86	3.63	3.48	3.37	3.29	3.23	3.18	3.14	3.07	3.01	2.94	2.90	2.86	2.83	2.79	2.75	2.71
10	4.96	4.10	3.71	3.48	3.33	3.22	3.14	3.07	3.02	2.98	2.91	2.85	2.77	2.74	2.70	2.66	2.62	2.58	2.54
11	4.84	3.98	3.59	3.36	3.20	3.09	3.01	2.95	2.90	2.85	2.79	2.72	2.65	2.61	2.57	2.53	2.49	2.45	2.40
12	4.75	3.89	3.49	3.26	3.11	3.00	2.91	2.85	2.80	2.75	2.69	2.62	2.54	2.51	2.47	2.43	2.38	2.34	2.30
13	4.67	3.81	3.41	3.18	3.03	2.92	2.83	2.77	2.71	2.67	2.60	2.53	2.46	2.42	2.38	2.34	2.30	2.25	2.21
14	4.60	3.74	3.34	3.11	2.96	2.85	2.76	2.70	2.65	2.60	2.53	2.46	2.39	2.35	2.31	2.27	2.22	2.18	2.13
15	4.54	3.68	3.29	3.06	2.90	2.79	2.71	2.64	2.59	2.54	2.48	2.40	2.33	2.29	2.25	2.20	2.16	2.11	2.07
16	4.49	3.63	3.24	3.01	2.85	2.74	2.66	2.59	2.54	2.49	2.42	2.35	2.28	2.24	2.19	2.15	2.11	2.06	2.01
17	4.45	3.59	3.20	2.96	2.81	2.70	2.61	2.55	2.49	2.45	2.38	2.31	2.23	2.19	2.15	2.10	2.06	2.01	1.96
18	4.41	3.55	3.16	2.93	2.77	2.66	2.58	2.51	2.46	2.41	2.34	2.27	2.19	2.15	2.11	2.06	2.02	1.97	1.92
19	4.38	3.52	3.13	2.90	2.74	2.63	2.54	2.48	2.42	2.38	2.31	2.23	2.16	2.11	2.07	2.03	1.98	1.93	1.88
20	4.35	3.49	3.10	2.87	2.71	2.60	2.51	2.45	2.39	2.35	2.28	2.20	2.12	2.08	2.04	1.99	1.95	1.90	1.84
21	4.32	3.47	3.07	2.84	2.68	2.57	2.49	2.42	2.37	2.32	2.25	2.18	2.10	2.05	2.01	1.96	1.92	1.87	1.81
22	4.30	3.44	3.05	2.82	2.66	2.55	2.46	2.40	2.34	2.30	2.23	2.15	2.07	2.03	1.98	1.94	1.89	1.84	1.78
23	4.28	3.42	3.03	2.80	2.64	2.53	2.44	2.37	2.32	2.27	2.20	2.13	2.05	2.01	1.96	1.91	1.86	1.81	1.76
24	4.26	3.40	3.01	2.78	2.62	2.51	2.42	2.36	2.30	2.25	2.18	2.11	2.03	1.98	1.94	1.89	1.84	1.79	1.73
25	4.24	3.39	2.99	2.76	2.60	2.49	2.40	2.34	2.28	2.24	2.16	2.09	2.01	1.96	1.92	1.87	1.82	1.77	1.71
26	4.23	3.37	2.98	2.74	2.59	2.47	2.39	2.32	2.27	2.22	2.15	2.07	1.99	1.95	1.90	1.85	1.80	1.75	1.69
27	4.21	3.35	2.96	2.73	2.57	2.46	2.37	2.31	2.25	2.20	2.13	2.06	1.97	1.93	1.88	1.84	1.79	1.73	1.67
28	4.20	3.34	2.95	2.71	2.56	2.45	2.36	2.29	2.24	2.19	2.12	2.04	1.96	1.91	1.87	1.82	1.77	1.71	1.65
29	4.18	3.33	2.93	2.70	2.55	2.43	2.35	2.28	2.22	2.18	2.10	2.03	1.94	1.90	1.85	1.81	1.75	1.70	1.64
30	4.17	3.32	2.92	2.69	2.53	2.42	2.33	2.27	2.21	2.16	2.09	2.01	1.93	1.89	1.84	1.79	1.74	1.68	1.62
40	4.08	3.23	2.84	2.61	2.45	2.34	2.25	2.18	2.12	2.08	2.00	1.92	1.84	1.79	1.74	1.69	1.64	1.58	1.51
60	4.00	3.15	2.76	2.53	2.37	2.25	2.17	2.10	2.04	1.99	1.92	1.84	1.75	1.70	1.65	1.59	1.53	1.47	1.39
120	3.92	3.07	2.68	2.45	2.29	2.17	2.09	2.02	1.96	1.91	1.83	1.75	1.66	1.61	1.55	1.50	1.43	1.35	1.25
∞	3.84	3.00	2.60	2.37	2.21	2.10	2.01	1.94	1.88	1.83	1.75	1.67	1.57	1.52	1.46	1.39	1.32	1.22	1.00

Table A.2 Percentiles of the t-distribution

f \ p	0.750	0.900	0.950	0.975	0.990	0.995	0.999
1	1.000	3.078	6.314	12.706	31.821	63.657	318
2	0.816	1.886	2.920	4.303	6.965	9.925	22.3
3	0.765	1.638	2.353	3.182	4.541	5.841	10.2
4	0.741	1.533	2.132	2.776	3.747	4.604	7.173
5	0.727	1.476	2.015	2.571	3.365	4.032	5.893
6	0.718	1.440	1.943	2.447	3.143	3.707	5.208
7	0.711	1.415	1.895	2.365	2.998	3.499	4.785
8	0.706	1.397	1.860	2.306	2.896	3.355	4.501
9	0.703	1.383	1.833	2.262	2.821	3.250	4.297
10	0.700	1.372	1.812	2.228	2.764	3.169	4.144
11	0.697	1.363	1.796	2.201	2.718	3.106	4.025
12	0.695	1.356	1.782	2.179	2.681	3.055	3.930
13	0.694	1.350	1.771	2.160	2.650	3.012	3.852
14	0.692	1.345	1.761	2.145	2.624	2.977	3.787
15	0.691	1.341	1.753	2.131	2.602	2.947	3.733
16	0.690	1.337	1.746	2.120	2.583	2.921	3.686
17	0.689	1.333	1.740	2.110	2.567	2.898	3.646
18	0.688	1.330	1.734	2.101	2.552	2.878	3.610
19	0.688	1.328	1.729	2.093	2.539	2.861	3.579
20	0.687	1.325	1.725	2.086	2.528	2.845	3.552
21	0.686	1.323	1.721	2.080	2.518	2.831	3.527
22	0.686	1.321	1.717	2.074	2.508	2.819	3.505
23	0.685	1.319	1.714	2.069	2.500	2.807	3.485
24	0.685	1.318	1.711	2.064	2.492	2.797	3.467
25	0.684	1.316	1.708	2.060	2.485	2.787	3.450
26	0.684	1.315	1.706	2.056	2.479	2.779	3.435
27	0.684	1.314	1.703	2.052	2.473	2.771	3.421
28	0.683	1.313	1.701	2.048	2.467	2.763	3.408
29	0.683	1.311	1.699	2.045	2.462	2.756	3.396
30	0.683	1.310	1.697	2.042	2.457	2.750	3.385
40	0.681	1.303	1.684	2.021	2.423	2.704	3.307
60	0.679	1.296	1.671	2.000	2.390	2.660	3.232
120	0.677	1.289	1.658	1.980	2.358	2.617	3.160
∞	0.674	1.282	1.645	1.960	2.326	2.576	3.090

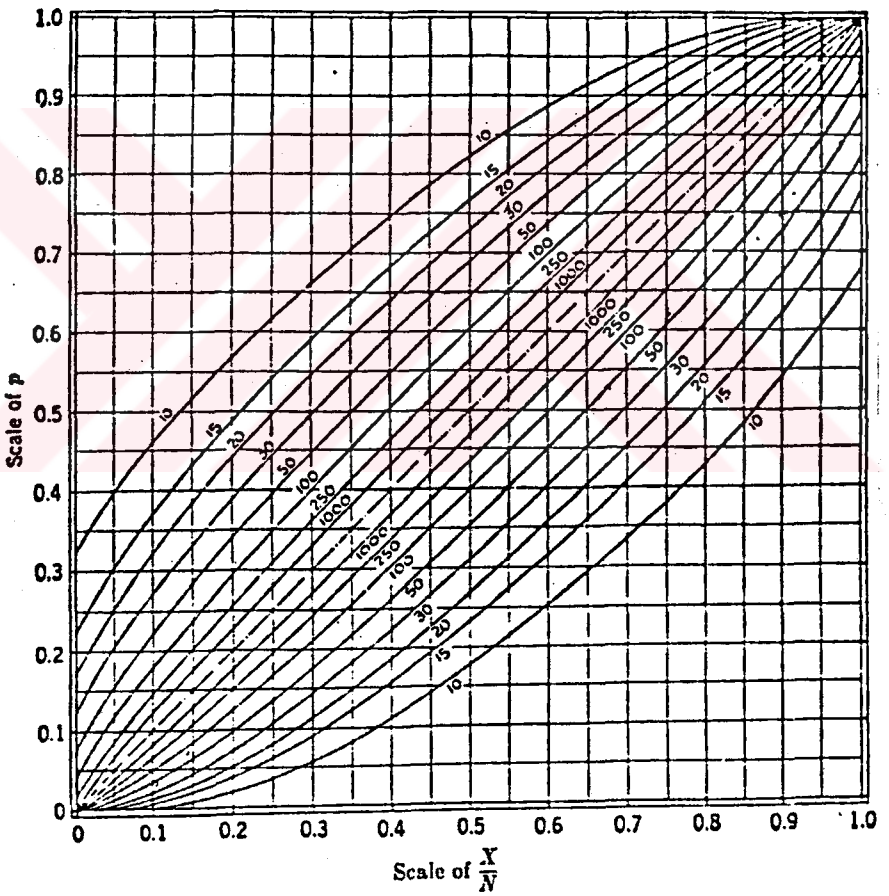

Figure A.1 Percentiles of the Binomial Distribution